

Figure 2 p27 binds to and colocalizes with Cdk5. **(a)** Lysates from COS7 cells transfected with indicated plasmids were immunoprecipitated (IP) and subsequently immunoblotted (WB) with indicated antibodies. NC, negative control; indicates immunoprecipitation with an anti-Myc antibody. **(b)** Purified p27, Cdk5 and p35 proteins were incubated *in vitro*, subsequently immunoprecipitated and immunoblotted with indicated antibodies. **(c)** Lysates

from cerebral cortices were immunoprecipitated with anti-p35 antibody and immunoblotted with anti-p27 antibody. **(d)** Primary cortical neurons were immunostained with anti-p27 (green) and anti-Cdk5 (red) antibodies. Scale bar, 16 μ m. **(e-h)** Higher magnification around neuronal soma **(f)** and process tip **(e)** of **d** and a growth cone **(g, h)** of another cell. Colocalization of p27 and Cdk5 (arrows). Scale bars, 4 μ m **(e, g)**, 0.5 μ m **(f, h)**.

shown). These findings indicate that Cdk5 is involved in protecting p27 against degradation via direct phosphorylation of p27 at Ser 10 in both primary cultured neurons and neurons in the developing brain.

Cdk5 binds to and colocalizes with p27

Our finding that Cdk5-p35 phosphorylates p27 raised a possibility that Cdk5-p35 may associate with p27. However, it was previously reported that Cdk5-p35 does not form a stable complex with p27, and eludes the CKI activity of p27 (ref. 24), indicating that interaction between Cdk5-p35 and p27 is probably transient or weak. To try to detect this interaction, the proteins were overexpressed in COS7 cells. When all three proteins were overexpressed, they could be coimmunoprecipitated with either anti-p27, Cdk5 or p35 antibody (Fig. 2a, lanes 1, 7, 9). However, in the absence of Cdk5, p27 and p35 could not be coimmunoprecipitated (lane 4), whereas the lack of p35 did not affect the coimmunoprecipitation of p27 and Cdk5 (lane 3). In addition, purified Cdk5-p35 complexes and p27 also coimmunoprecipitated when they were mixed *in vitro* (Fig. 2b). These results indicate that p27 can directly bind to Cdk5 but not p35. Furthermore, Cdk5 did not coimmunoprecipitate with a mutant p27 protein (W60G) in which Trp60 was substituted with Gly and known to

not bind Cdk2 (ref. 25), indicating that interaction probably occurs at the common CDK binding region (Fig. 2a, lane 5). Accordingly, endogenous p27, as well as Cdk5, coimmunoprecipitated with p35 from E16 cerebral cortical lysate, although this interaction seems to be relatively weak (Fig. 2c). This result indicates that these three proteins form a complex in post-mitotic neurons in the developing cerebral cortex, because p35 is expressed in post-mitotic neurons but not in proliferating precursor cells⁷. In addition, this weak interaction between Cdk5-p35 and p27 *in vivo* may explain the phosphorylation of p27 by Cdk5 but its ability to avoid p27 CKI activity²⁴. These results were also supported by a recent biochemical analysis that showed direct but weak interaction between Cdk5 and p27 *in vitro*²⁶.

Next, we investigated the subcellular localization of p27 in primary cultured neurons from E15 cerebral cortices. Immunocytochemistry revealed not only nuclear localization but also punctate cytoplasmic expression (Fig. 2d). p27 punctate staining was abundantly observed in the perinuclear regions and the tips of processes, where accumulation of Cdk5 signals was also observed (Fig. 2d). At high magnification, overlap between the punctate p27 and Cdk5 signals could be observed in the perinuclear regions (Fig. 2f, arrows) and the process tips (arrows in Fig. 2e, g, h). Together with the

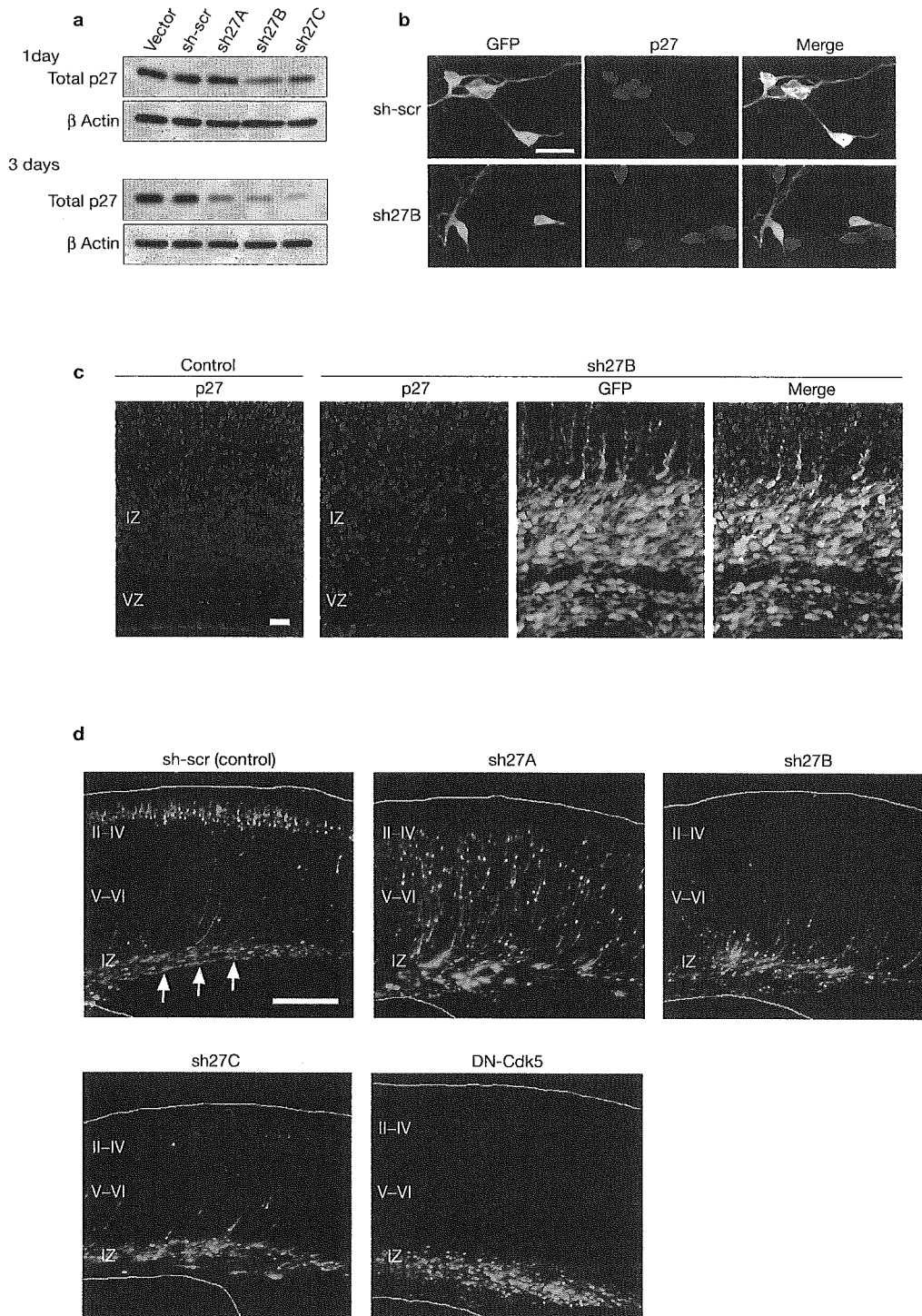


Figure 3 Effects of p27 shRNAs. (a) Amount of p27 in primary cortical neurons transfected with indicated shRNA vectors. (b) Primary cortical neurons introduced with sh27B. p27 signal (red) was weakened in transfected GFP-positive cells (2DIV). (c) Embryonic brains electroporated with sh27B or control plus EGFP, followed by fixation at E17, subsequently

coimmunoprecipitation data, this indicates that p27 associates with Cdk5 in those regions of cortical neurons, probably in a transient manner.

p27 is involved in neuronal migration

To deplete endogenous p27 in neurons, three shRNA-expressing vectors (sh27A, sh27B and sh27C) were designed to target distinct regions in

subjected to immunostaining with indicated antibodies. IZ, intermediate zone; VZ, ventricular zone. (d) Post-natal day (P) 0 brains electroporated with indicated vectors plus EGFP at E14. Arrows indicate the neurite bundles in the intermediate zone. II–IV, layers II–IV of the cortical plate; V–VI, layers V–VI of the cortical plate. Scale bars, 20 μ m (b, c), 200 μ m (d).

the p27 coding sequence. These shRNA vectors were introduced into primary cortical neurons from E14 embryos to estimate the effectiveness of each construct in decreasing p27 levels. The transfection efficiency was $91.52 \pm 2.10\%$ in our experimental conditions (see Supplementary Information, Fig. S3b). One day after transfection, sh27B and sh27C were seen to mildly decrease the amount of p27 compared with control

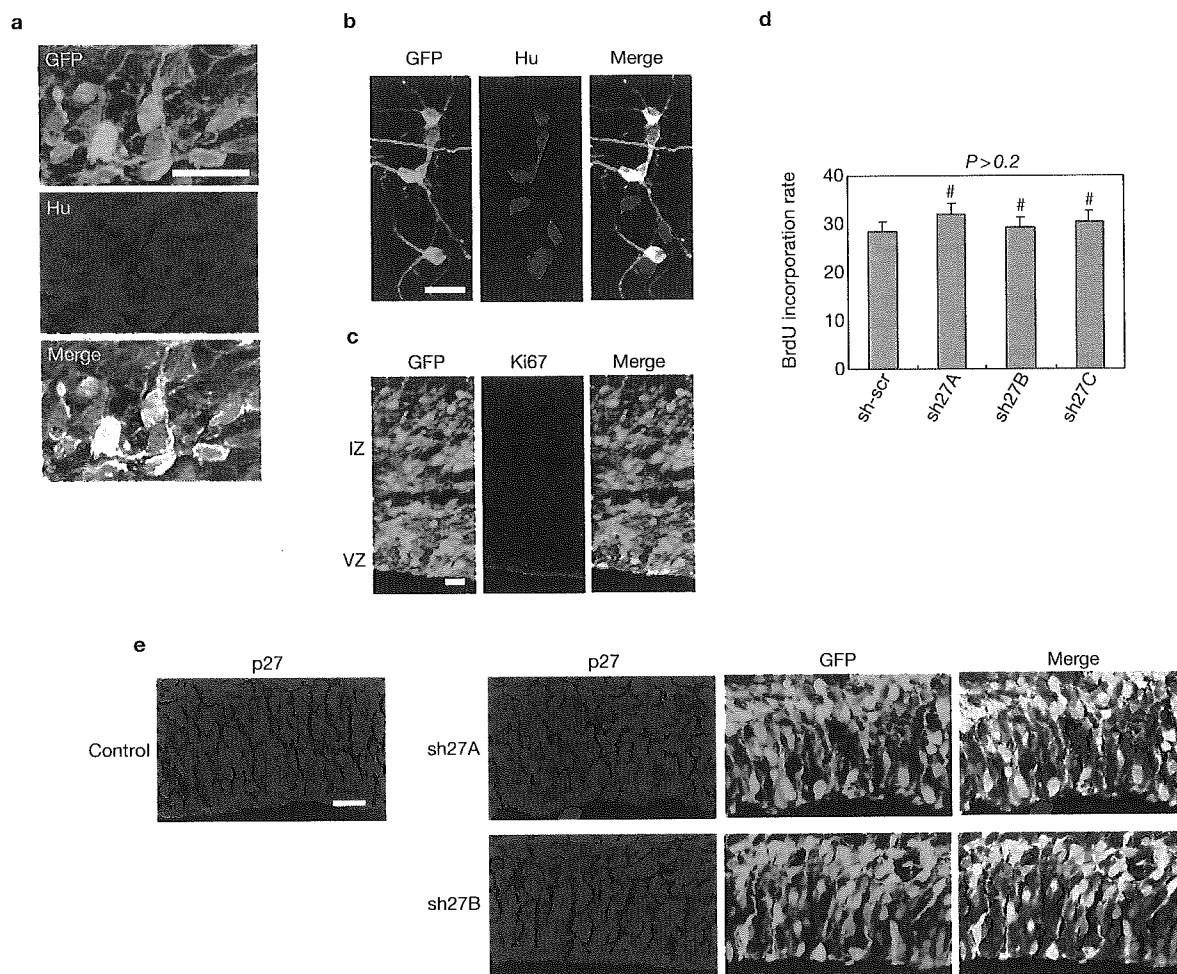


Figure 4 Effects of p27 shRNAs on cell cycle and differentiation.

(a, c) Embryonic brains were electroporated with sh27B plus enhanced GFP, followed by fixation at E17 and, subsequently, subjected to immunostaining with indicated antibodies. IZ, intermediate zone; VZ, ventricular zone. (b) Primary cortical neurons were transfected with sh27B plus EGFP (2DIV) and immunostained with indicated antibodies. (d) BrdU incorporation rates of transfected cells in the ventricular zone of E15 cortices, which were

electroporated with indicated vectors plus EGFP at E14. (e) Embryonic brains were electroporated with indicated vectors plus EGFP, followed by fixation at E15 and, subsequently, subjected to immunostaining with indicated antibodies. The effect of sh27A was suppressed by coelectroporation with a human p27-expressing vector, the expression of which is not suppressed by sh27A due to the diverse DNA sequence in that region (data not shown). Scale bars, 20 μ m (a-c, e).

scrambled-shRNA (sh-scr), whereas sh27A had little effect. At 3 d post-transfection, all three vectors decreased the amount of p27 (Fig. 3a). The effectiveness of the RNA interference seemed to be stronger for sh27B and sh27C, and weaker for sh27A (Fig. 3a). A decrease in p27 protein levels was also observed by immunocytochemistry in primary cortical neurons (2DIV), which were transfected with sh27B (Fig. 3b). The ratio of p27-positive cells to transfected cells was prominently reduced to $17.92 \pm 3.41\%$ (see Supplementary Information, Fig. S3a). Next, E14 cerebral cortices were electroporated *in utero* with each shRNA vector plus pEGFP¹⁹ and examined after 3 d. Significant reduction of p27 protein was observed in cells transfected with any of the vectors (Fig. 3c for sh27B, and data not shown for the other vectors), indicating the efficiency of the p27 shRNAs in electroporated animals.

Cdk5 is known to have essential roles in neuronal migration during the development of the cerebral cortex through its kinase activity^{6,7,19,20}. The notion that Cdk5 phosphorylates and stabilizes p27 in developing cortical neurons raises the possibility that p27 may also be involved in cortical neuronal migration as one of the downstream phosphorylation

targets of Cdk5. To investigate whether p27 is required for normal neuronal migration, shRNA vectors were electroporated *in vivo* into E14 cerebral cortices and the consequences were observed at post-natal day 0 (P0), 5 d after electroporation. Whereas most sh-scr-transfected cells migrated normally to the superficial layer of the cortical plate, sh27B- and sh27C-transfected cells remained in the intermediate zone (Fig. 3d, and see Supplementary Information, Fig. S4). Many sh27A-transfected cells were also observed in the intermediate zone, although a portion of the transfected cells reached the cortical plate, probably due to the weaker RNAi effect of sh27A (Fig. 3d). Because these shRNAs were targeted against distinct regions of the p27 coding sequence, the abnormal positioning of shRNA-introduced cells is probably a result of the suppression of p27 protein levels, rather than a non-specific effect.

Because neural precursors proliferate only in the ventricular zone (or subventricular zone), cells in the intermediate zone, which are derived from the precursors, should be post-mitotic neurons. At 3 d after electroporation, many of the sh27B-electroporated cells had migrated out of the ventricular zone (Fig. 3c) and were expressing a

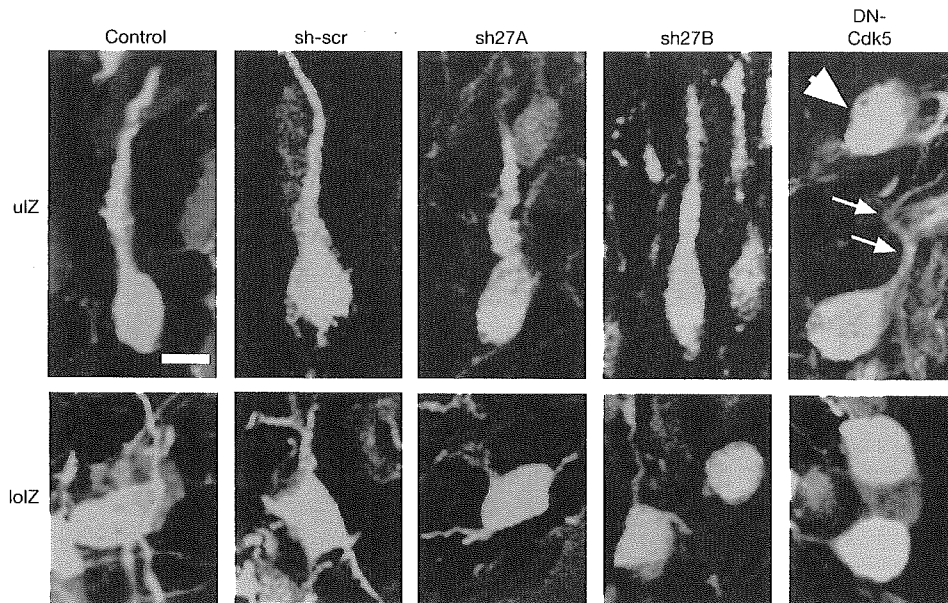


Figure 5 Effects of p27 shRNAs on morphology of migrating neurons. E17 brains that were electroporated with indicated vectors at E14. High

magnification of upper intermediate zone (uIZ) or lower intermediate zone (loIZ). Scale bar, 5 μ m.

neuronal marker, Hu (Fig. 4a), but were not expressing the proliferating markers Ki67 (Fig. 4c) and proliferating cell nuclear antigen (PCNA) (see Supplementary Information, Fig. S3c). Accordingly, when primary cortical neurons were transfected with sh27B and cultured for 2 d, few PCNA-positive cells were observed (see Supplementary Information, Fig. S3d). Most transfected cells were Hu-positive (Fig. 4b), although the amount of p27 was extremely low in those cells (Fig. 3b). This indicates that sh27B-introduced cells differentiate normally into post-mitotic neurons and do not re-enter the cell cycle after exiting from the ventricular zone. To further examine whether shRNAs for p27 affect proliferation of neural precursors in the ventricular zone, we analysed shRNA-introduced brains 1 d post-electroporation, when most of the shRNA-introduced cells were found in the ventricular zone. At this stage, sh27A or sh27B barely affected the expression level of p27 in the transfected ventricular zone cells (Fig. 4e). Next, E14 embryos were electroporated with p27-shRNAs, subjected to intraperitoneal injections of bromodeoxyuridine (BrdU) at E15 (see Methods), and dissected 1 h after the first injection. The BrdU incorporation rates of transfected cells in the ventricular zone were not significantly affected by either shRNA (Fig. 4d). In addition, the positions of transfected and/or BrdU-incorporated cells within the ventricular zone were not affected (see Supplementary Information, Fig. S3e). Considering that some of ventricular zone cells move up and down within the ventricular zone in accordance with their cell-cycle status³, these findings indicate that the cell cycle of the ventricular-zone cells were not affected at 1 d after electroporation, probably because the shRNA constructs could not effectively reduce the endogenous p27 within this time period, as indicated in Fig. 4e. These results indicate that the stalled effect of the shRNA-transfected cells (Fig. 3d, and see Supplementary Information, Fig. S4) are caused by an abnormality in cell migration, rather than secondary effects of disorganized differentiation or proliferation. These phenotypes, observed in shRNA-introduced brains, were similar to those in DN-Cdk5-electroporated brains, in which targeted cells could not migrate into the cortical plate (Fig. 3d, and see Supplementary

Information, Fig. S4). These results imply that p27 acts downstream of Cdk5, which contributes to proper neuronal migration.

Newly-born neurons generated from the ventricular zone primarily exhibit multipolar morphology in the lower part of the intermediate zone (loIZ) and, subsequently, transform into spindle-like shapes with a leading process, entering into the upper intermediate zone (uIZ) to migrate towards the pial surface^{27,28}. Three days post-electroporation (E17), the morphology of EGFP-electroporated neurons can be observed both in the loIZ and uIZ under our experimental conditions (Fig. 5, control). Interestingly, cells in the loIZ that were electroporated with sh27B or DN-Cdk5 did not exhibit the normal multipolar shape but were relatively round, with thin processes (Fig. 5, lower panels), with a milder effect being observed for sh27A. This indicates that Cdk5 and p27 participate in regulating the multipolar morphology of neurons in the loIZ. In the uIZ, DN-Cdk5-introduced cells often lost their leading process (Fig. 5, arrowhead) or possessed an abnormal one (Fig. 5, arrows). By contrast, the morphology of sh27A- or 27B-transfected neurons seemed unaffected in the uIZ (Fig. 5, upper panels), although they could not migrate into the cortical plate (Fig. 3d, and see Supplementary Information, Fig. S4). These results indicate that p27 is involved in the regulation of cell morphology in the loIZ, as well as cell migration into the cortical plate, but does not affect the leading process formation in the uIZ; Cdk5, on the other hand, participates in all of these events. As Cdk5 phosphorylates other molecules (for example, FAK, Nudel and doublecortin), which are also implicated in neuronal migration^{3,7,29,30}, some of those molecules may be involved in the leading process formation in the uIZ.

Cdk5-p27 regulates cofilin activity

Costaining with an anti-p27 antibody and phalloidin revealed colocalization of p27 with F-actin in cultured neurons from E15 cerebral cortices, particularly at process tips (Fig. 6a). This raised the possibility that a Cdk5-p27 pathway may be involved in regulating cytoskeletal actin. To investigate the role of p27 in actin reorganization *in vivo*, we coelectroporated sh27B- and EGFP-actin-expressing plasmids into E14 cortices, and

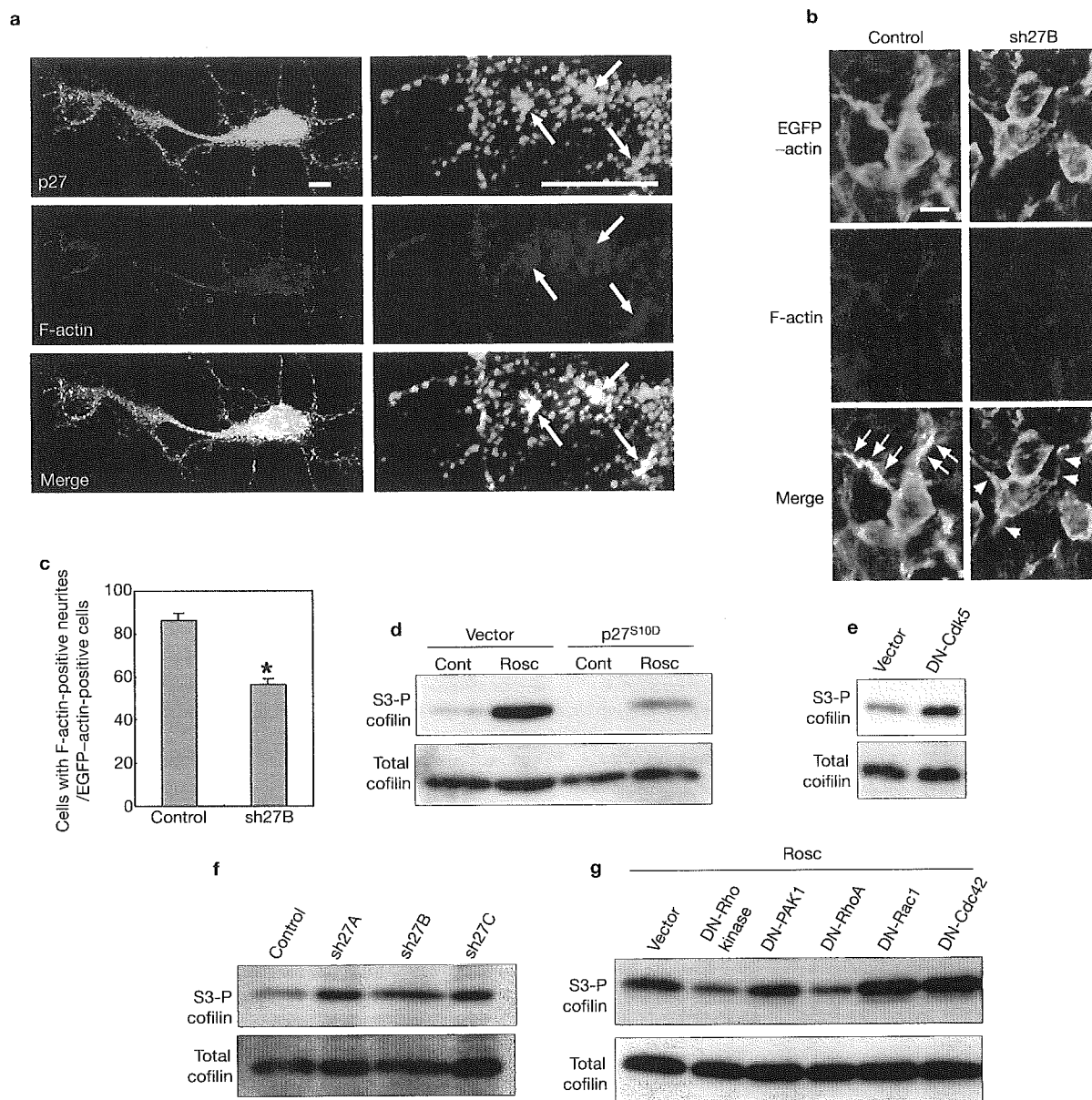


Figure 6 Cdk5 and p27 control cofilin phosphorylation. (a) Localization of p27 (green) and F-actin (red) in primary cortical neurons. Right panels: higher magnifications of process tip, showing colocalization (arrows). (b) Multipolar cells in lower intermediate zone (loIZ) coelectroporated with sh27B plus EGFP-actin vectors at E14 and fixed at E17. (c) Quantitative analysis of b. Ratios of

cells with F-actin-positive neurites/EGFP-actin-positive cells are shown. (d-g) Immunoblot analyses of primary cortical neurons transfected with indicated vectors (2DIV in d, f, g; 5DIV in e). In g, increase of cofilin Ser3 phosphorylation is suppressed by DN-RhoA or DN-ROCK. DN-Rac1 or DN-Cdc42, in contrast, caused a mild increase of phosphorylation. Scale bar, 6 μ m (a, b).

examined the brains at E17. In the control brains, strong F-actin signals were observed in the processes of multipolar cells in the loIZ (Fig. 6b, arrows). However, significantly less F-actin signals were observed in sh27B-electroporated processes, which contained abundant G-actin, as deduced from the EGFP-actin signals (Fig. 6b, arrowheads). Accordingly, the ratio of transfected cells in the loIZ, which possessed at least one F-actin-positive neurite, was significantly reduced in sh27B-electroporated brains (Fig. 6c). These findings indicate that p27 is involved in regulating actin cytoskeletal organization in migrating neurons.

Given that the Cdk5-p27 pathway can affect actin cytoskeleton in neurons, we focused on cofilin, an actin-binding protein, which regulates actin reorganization via its actin-severing activity. The activity of cofilin is regulated through its phosphorylation at Ser 3; Ser 3 non-phosphor-

ylated and phosphorylated forms are active and inactive, respectively^{31,32}. Our experiment showed that treatment of primary cultured neurons with roscovitine increased Ser 3 phosphorylation of cofilin (Fig. 6d, lanes 1, 2), indicating that Cdk5 negatively regulates this phosphorylation. Interestingly, this roscovitine-enhanced phenomenon was suppressed by overexpression of p27^{S10D}, a stable form of p27 (Fig. 6d, lanes 3, 4). By contrast, this roscovitine-enhanced phenomenon was not markedly suppressed by p27^{S10A}, an unstable form of p27 (see Supplementary Information, Fig. S5d). In p27^{S10A}-transfected cortical cultures, p27 levels were significantly reduced, as expected (data not shown). These findings indicate that p27 acts downstream of Cdk5 with regards to Ser 3 phosphorylation of cofilin, and further indicates that Cdk5 suppresses Ser 3 phosphorylation of cofilin by increasing the amount of p27 via

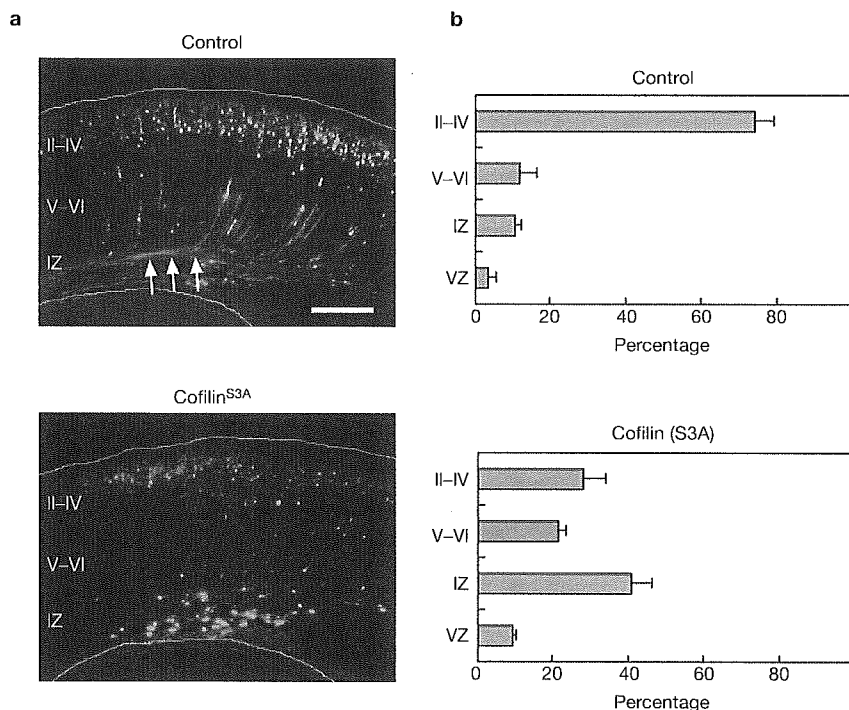


Figure 7 Cofilin^{S3A} disturbed neuronal migration. (a) Effect of electroporation of cofilin^{S3A} into E14 cerebral cortices. Brains were fixed at P0. Scale bar, 200 μ m.

(b) Estimation of cell migration ($n=5$)¹⁹. II-IV, layers II-IV of the cortical plate; V-VI, layers V-VI of the cortical plate; IZ, intermediate zone; VZ, ventricular zone.

Ser 10 phosphorylation. Negative regulation of cofilin phosphorylation by Cdk5 and p27 was supported by the observations that expression of DN-Cdk5 and p27-shRNAs also increased the Ser 3 phosphorylation of cofilin (Fig. 6e, f).

In fibroblasts, a recent report showed that p27 suppresses the activity of the RhoA-ROCK (Rho-kinase) pathway, thereby decreasing Ser 3 phosphorylation of cofilin³³. Cofilin is directly phosphorylated by LIMK, the activities of which are known to be regulated not only by ROCK (Rho-kinase) but also by PAK1 (ref. 31), and this PAK1 activity can also be regulated by Rac1 and Cdc42 (ref. 31). To determine which signalling pathway is involved in cofilin phosphorylation downstream of Cdk5, dominant-negative forms of candidate molecules were transfected to cultured cortical neurons (Fig. 6g). We found that Ser 3 phosphorylation of cofilin induced by roscovitine was suppressed by DN-ROCK (Rho-kinase) and DN-RhoA but not by DN-PAK1, DN-Rac1 or DN-Cdc42. These results indicate that this event does not involve the Rac1-PAK1 or Cdc42-PAK1 pathways, but rather the RhoA-ROCK (Rho-kinase) pathway. Consistently, the increment of cofilin phosphorylation induced by roscovitine was also suppressed by Y27632, an inhibitor for ROCK (Rho-kinase) (see Supplementary Information, Fig. S5c). This notion is also supported by our immunocytochemical study that p27 and RhoA were colocalized at process tips in cultured cortical neurons (see Supplementary Information, Fig. S5a, b).

S3A-cofilin disturbs neuronal migration

To investigate the importance of cofilin phosphorylation in cortical neuronal migration, a mutant cofilin^{S3A}, the Ser 3 of which was replaced with Ala³², was electroporated into the developing cerebral cortices at E14. At P0, 5 d after electroporation, many cofilin^{S3A}-electroporated cells were observed in the intermediate zone, whereas most of the control-transfected cells were located in the superficial layer of the cortical plate (Fig. 7a, b).

Because the overexpressed cofilin^{S3A} cannot be phosphorylated at the Ala3 site, this result indicates that an appropriate balance of Ser 3 phosphorylation of cofilin may be required for proper cortical neuronal migration.

DISCUSSION

In general, CKIs suppress CDK activities as upstream regulators of the cell cycle in proliferating cells⁸. Whereas Cdk2-cyclin E is known to negatively regulate p27^{kip1} during S phase^{8,34}, our findings indicate that p27 function is positively regulated as a downstream target of Cdk5 in neurons, implicating that a new relationship exists between CDKs and CKIs in G0-arrested cells. Cdk5 stabilizes and increases p27 protein through Ser 10 phosphorylation, which eventually contributes to neuronal migration in the developing cerebral cortex (Fig. 8). On the other hand, previous studies have revealed that proliferating neural precursors in the cortical ventricular zone require the CKI activity of p27 for proper cell-cycle regulation^{9,10,35}. These facts indicate that p27^{kip1} has dual roles in successive developmental events during corticogenesis: regulation of the cell cycle in ventricular-zone cells and migration of post-mitotic neurons.

Although several studies reported that Cdk5 regulates microtubules via phosphorylation of FAK, Nudel and doublecortin^{3,7,29,30}, it was unclear whether Cdk5 controls actin cytoskeleton in the developing cortex. In this study, we show that Cdk5 and p27 suppress Ser 3 phosphorylation of an actin-binding protein, cofilin, and that suppression of p27 resulted in decreased F-actin levels in migrating neuronal processes. These findings indicate that the Cdk5-p27 pathway controls the actin cytoskeleton to regulate neuronal migration (Fig. 8).

Although several *in vitro* studies have indicated the involvement of p27 in cell migration^{16,33,36,37}, the physiological relevance of p27 has remained elusive. Actually, p27-deficient mice did not display any obvious migration-defect-related phenotypes^{11-13,36}. Previous studies reported few abnormalities in p27^{kip1}- or p57^{kip2} (another p27 CKI member)-deficient

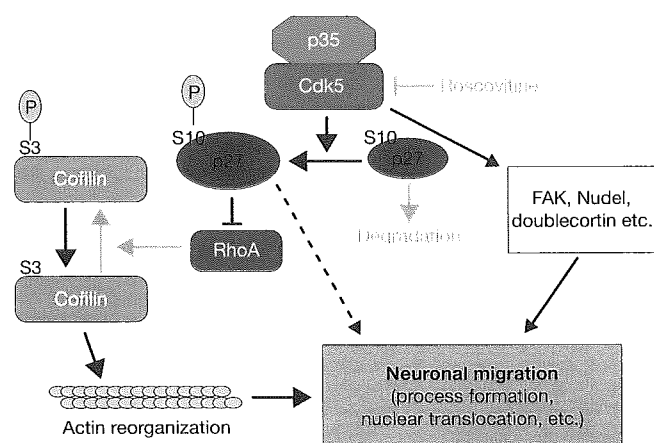


Figure 8 A model for the role of Cdk5 and p27 in cortical neuronal migration. Cdk5 stabilizes p27 by phosphorylating the Ser 10 site, eventually increasing the amount of p27 protein. It leads to an increase of non-phosphorylated, activated cofilin through the suppression of RhoA activity, which may be required for actin cytoskeletal reorganization in the processes of migrating neurons. Together with previous reports that Cdk5 regulates microtubule organization via phosphorylating FAK, doublecortin and the Nudel–Lis1 complex^{3,7,29}, Cdk5 may coordinate both actin and microtubules to promote cortical neuronal migration.

mice in tissues that express both p27 and p57 (ref. 38). We observed that both p27 and p57 were expressed in migrating neurons in the intermediate zone (see Supplementary Information, Fig. S3f). Together with the fact that p57 was also shown to regulate the RhoA–cofilin pathway³⁶, p57 may compensate for the function of p27 in migrating neurons of p27-deficient mice. It has been suggested that *in utero* electroporation technique allows us to conditionally and acutely suppress protein function, which may circumvent the compensation effects of general gene-knockout approaches^{19,29,30,39}. The advantage of this method was shown in the case of *doublecortin*^{39,40}, a causative gene of lissencephaly, the shRNA of which caused abnormal neuronal migration resembling human lissencephaly, whereas *Doublecortin*-deficient cerebral cortices exhibited no obvious abnormality⁴¹. In this study, this technique also seems to uncover a hidden phenotype — that is, the neuronal migration defect in p27-deficient mice. □

METHODS

Plasmids. Plasmids were prepared using the Endo Free plasmid purification kit (Qiagen, Valencia, CA). wt- and DN-Cdk5 (refs 19, 20), p35 (ref. 20), HA-tagged wt-, p27^{S10D} and p27^{S10A} (ref. 14), HA-tagged p27^{W60G} (ref. 25), cofilin^{S3A} (ref. 32), DN-RhoA⁴², DN-Rac1 (ref. 19), DN-Cdc42 (ref. 42), DN-ROCK (Rho-kinase)⁴³, DN-PAK1 (ref. 44) and EGFP–actin (Clontech, Mountain View, CA) cDNA were inserted into pCAG–MCS2 vectors²⁰. EGFP was described previously¹⁹. To construct shRNA-expressing vectors, oligonucleotides targeting three distinct regions in the p27 coding sequence (sh27A: 5'-GGTCAATCATGAAGAACCTA-3'; sh27B: 5'-AGACAATCAGGCTGGGTTA-3'; sh27C: 5'-GAAGCGACCTGCTGCAGAA-3'); two distinct regions in the *Cdk5* coding sequence (shCK5A: 5'-GAACTGTGTTCAAGGCTAA-3' and sh27B: 5'-GATCAGGACCTGAAGAAAT-3'); a control scrambled sequence (sh-scr: 5'-TACGCGCATAAGATTAGGG-3') and their complementary sequences were inserted into the mU6pro vector⁴⁵. All contain a nine-base hairpin loop sequence (5'-TTCAAGAGA-3'). These sequences were designed based on information from shRNA sequence analyses (B-Bridge International, Inc., Sunnyvale, CA). The mU6 promoter in the mU6pro vector was reported to drive efficient expression of shRNA in the developing cerebral cortex when introduced by *in utero* electroporation³⁹.

Antibodies and chemical reagents. Primary antibodies used in this study were anti-phospho-Ser 10 p27 (Zymed, South San Francisco, CA), anti-phospho-Thr187 p27 (Zymed), anti-p27 (BD Transduction Laboratories, San Jose, CA; Santa Cruz (Santa Cruz, CA); C-19, N-20), anti- β -actin (AbCam, Cambridge, UK), anti- β -tubulin (Sigma, St Louis, MO), anti-GFP (Molecular Probes, Eugene, OR), anti-HA (Upstate Biotechnology, Charlottesville, VA), anti-Cdk5 (Santa Cruz; J-3, C-8), anti-p35 (Santa Cruz; C-19), anti-Hu (Molecular Probes), anti-Ki67 (Novocastra, Newcastle upon Tyne, UK), anti-PCNA (BD Transduction Laboratories), anti-p57 (Santa Cruz; H-91), anti-Cdk2 (Santa Cruz; H-298), anti-Cdc2 (Santa Cruz; C-19), anti-RhoA (Santa Cruz; 26C4), anti-phospho-Ser 3 cofilin (Chemicon, Temecula, CA; Santa Cruz) and anti-cofilin (Cell Signaling, Beverly, MA; AbCam) antibodies. Specificity of anti-phospho-Ser 10 antibody was confirmed by the inability to recognize mutant p27^{S10A} (Fig. 1a). Roscovitine was purchased from Sigma; Y27632 and U0126 were purchased from Calbiochem (San Diego, CA); and SP600125 and MG132 were purchased from Biomol International (Plymouth Meeting, PA). Inhibitors were used at final concentrations of 100 μ M (roscovitine), 50 μ M (SP600125) and 10 μ M (MG132), except where otherwise indicated in Supplementary Information Figs 1 and 5.

Cell culture and transfection in COS7 cells. COS7 cells were maintained in Dulbecco modified Eagle's medium (Invitrogen, Carlsbad, CA) with 10% fetal bovine serum (FBS) and antibiotics²⁰. Plasmids were transfected into COS7 cells using a Lipofectamine Plus reagent kit (Invitrogen) in Opti-MEM (Invitrogen), according to the manufacturer's instructions. After 3 h incubation, fresh medium containing 10% FBS was substituted, and cells were cultured for a subsequent 24 h.

***In utero* electroporation and slice culture of embryonic cerebral cortex.** Pregnant ICR mice were purchased from SLC Japan (Sizuoka, Japan). p35-deficient mice were purchased from Jackson Laboratory (Bar Harbour, ME). Animals were handled in accordance with guidelines established by Kyoto University. All electroporations in this report were performed on E14 embryos. *In utero* electroporation, quantification of EGFP fluorescence intensities in various regions of electroporated cerebral cortices, and slice cultures of E16 mouse cerebral cortices were performed, as described previously^{19,20}.

Quantitative estimation of p27-positive cells in DN-Cdk5 introduced brains (Fig. 1g). E14 embryos were co-electroporated with DN-Cdk5 or control vector plus EGFP, and dissected at E17. Frozen sections were immunostained with anti-GFP (green) and anti-p27 (red) antibodies (Fig. 1f). Relative fluorescence intensities of p27 in GFP-positive areas to GFP-negative areas were measured in control and DN-Cdk5 electroporated brains, respectively, with Leica TCL SP2 software. The mean relative fluorescence intensity in control brains was scored "100".

Primary culture of embryonic cerebral cortex, and transfection. E15 mouse embryonic cerebral cortices were treated with 0.25% Trypsin-EDTA for 15 min at 37°C and dissociated into single cells by gentle trituration. Cells were suspended in 500 μ l of Neurobasal medium (Invitrogen) supplemented with B27 (Invitrogen) and 2 mM L-glutamine (Sigma), and then plated at a density of about 10,000 cells/cm² on coverslips coated with 1 mg ml⁻¹ poly-D-lysine (Sigma) in a six-well plate. Transfections into primary cultures of E15 cerebral cortices were performed using Amaxa mouse neuron nucleofector kit (Amaxa Biosystems, Cologne, Germany), according to the manufacturer's instructions. The efficiency of transfection was estimated to be 91.52 \pm 2.10% under our experimental conditions (see Supplementary Information, Fig. S3b).

Immunoblot analysis and immunocytochemistry. Cell and tissue lysates in SDS sample buffer (50 mM Tris-HCl (pH 6.8), 2% SDS, 10% glycerol, 100 mM DTT (dithiothreitol) and Bromophenol Blue) were separated with SDS-PAGE and electrophoretically transferred onto polyvinylidene difluoride (PVDF) membranes. Membranes were blocked with 5% skimmed milk in TBST (20 mM Tris-HCl (pH 7.5), 150 mM NaCl and 0.05% Tween20) for 1 h and probed with primary antibodies in 5% skimmed milk in TBST or Can Get Signal reagents (Toyobo, Osaka, Japan), followed by treatment with horseradish-peroxidase-conjugated secondary antibodies and ECL Plus Western blotting detection reagents (Amersham, Piscataway, NJ). Signals were detected and measured with a cooled charge-coupled device camera (LAS-3000mini; Fuji-firm, Tokyo, Japan). Immunocytochemistry was performed as described previously^{46–48}.

Immunoprecipitation and *in vitro* binding assay. Transfected COS7 cells were lysed with buffer (1% Triton X-100, 20 mM Tris-HCl (pH 7.5), 150 mM NaCl, protease inhibitor mix (Roche, Basel, Switzerland), 50 mM NaF, 1 mM orthovanadate, 5 mM pyrophosphate and 10 mM β -glycerophosphate). Cell lysates were incubated with anti-Cdk5 or anti-p35 or anti-p27 antibody at 4°C for 90 min, followed by additional incubation with protein G-Sepharose (Amersham Pharmacia, Piscataway, NJ) for 90 min. The beads were washed five times with phosphate-buffered saline (PBS), and bound proteins were analysed by SDS-PAGE and immunoblot analysis as described above. For lysate from E16 mouse embryonic cerebral cortices, 1% Nonidet P-40 was used, instead of 1% Triton X-100. *In vitro* binding assay was performed as described elsewhere⁴⁹. Briefly, purified Cdk5-p35 complex expressed in insect cells (Invitrogen Panvera, Carlsbad, CA) and p27 expressed in *Escherichia coli* (Santa Cruz) were incubated in PBS containing 1% Triton X-100 at 4°C for 60 min. Then, the mixture was immunoprecipitated with the anti-p27 antibody, and bound proteins were analysed by SDS-PAGE and immunoblot analysis.

***In vitro* kinase assay.** Purified Cdk5-p35 complex (Invitrogen Panvera) and p27 (Santa Cruz) were incubated in 50 μ l of kinase buffer (50 mM Tris-HCl (pH 7.5), 10 mM MgCl₂, 200 μ M ATP, 1 mM DTT) at 30°C for 30 min. The mixture was subjected to immunoblot analysis with antibodies against phosphorylated and total p27.

Immunohistochemistry and BrdU incorporation experiment. Immunohistochemistry and BrdU incorporation experiments were performed as described previously¹⁹. For F-actin staining, rhodamine-phalloidin (Molecular Probes) was incubated with an Alexa488-conjugated secondary antibody (Molecular Probes).

Note: Supplementary Information is available on the Nature Cell Biology website.

ACKNOWLEDGEMENTS.

We thank G. Bokoch, K. Kaibuchi, S. Meloche, K. Moriyama, M. Nakanishi, A. Takashima, L.H. Tsai and D.L. Turner for providing plasmids. We also thank K-i. Nakayama, K. Nakayama, R. Yu and M. Sone for helpful comments. This work was supported by the Center of Excellence (COE) grant and Grant-in-Aid for Scientific Research on Priority Areas, "Elucidation of glia-neuron network mediated information processing systems (#16047220)", "Molecular Brain Science 16067101 (#17024030)" and "Membrane Traffic" from the Ministry of Education, Culture, Sports, and Science and Technology, Japan, and by grants from Japan Brain Foundation and Takeda Science Foundation.


COMPETING FINANCIAL INTERESTS

The authors declare that they have no competing financial interests.

Published online at <http://www.nature.com/naturecellbiology/>

Reprints and permissions information is available online at <http://npg.nature.com/reprintsandpermissions/>

- Sherr, C. J. & Roberts, J. M. Living with or without cyclins and cyclin-dependent kinases. *Genes Dev.* **18**, 2699–2711 (2004).
- Massague, J. G1 cell-cycle control and cancer. *Nature* **432**, 298–306 (2004).
- Bielas, S., Higginbotham, H., Koizumi, H., Tanaka, T. & Gleeson, J. G. Cortical neuronal migration mutants suggest separate but intersecting pathways. *Annu. Rev. Cell Dev. Biol.* **20**, 593–618 (2004).
- Mochida, G. H. & Walsh, C. A. Molecular genetics of human microcephaly. *Curr. Opin. Neurol.* **14**, 151–156 (2001).
- Tsai, L. H., Takahashi, T., Caviness, V. S. Jr & Harlow, E. Activity and expression pattern of cyclin-dependent kinase 5 in the embryonic mouse nervous system. *Development* **119**, 1029–1040 (1993).
- Gilmore, E. C., Ohshima, T., Goffinet, A. M., Kulkarni, A. B. & Herrup, K. Cyclin-dependent kinase 5-deficient mice demonstrate novel developmental arrest in cerebral cortex. *J. Neurosci.* **18**, 6370–6377 (1998).
- Gupta, A., Tsai, L. H. & Wynshaw-Boris, A. Life is a journey: a genetic look at neocortical development. *Nature Rev. Genet.* **3**, 342–355 (2002).
- Sherr, C. J. & Roberts, J. M. CDK inhibitors: positive and negative regulators of G1-phase progression. *Genes Dev.* **13**, 1501–1512 (1999).
- Goto, T., Mitsuhashi, T. & Takahashi, T. Altered patterns of neuron production in the p27 knockout mouse. *Dev. Neurosci.* **26**, 208–217 (2004).
- Tarui, T. *et al.* Overexpression of p27Kip1, probability of cell cycle exit, and laminar destination of neocortical neurons. *Cereb. Cortex* **15**, 1343–1355 (2005).
- Fero, M. L. *et al.* A syndrome of multiorgan hyperplasia with features of gigantism, tumorigenesis, and female sterility in p27(Kip1)-deficient mice. *Cell* **85**, 733–744 (1996).
- Kiyokawa, H. *et al.* Enhanced growth of mice lacking the cyclin-dependent kinase inhibitor function of p27(Kip1). *Cell* **85**, 721–732 (1996).
- Nakayama, K. *et al.* Mice lacking p27(Kip1) display increased body size, multiple organ hyperplasia, retinal dysplasia, and pituitary tumors. *Cell* **85**, 707–720 (1996).
- Rodier, G. *et al.* p27 cytoplasmic localization is regulated by phosphorylation on Ser10 and is not a prerequisite for its proteolysis. *EMBO J.* **20**, 6672–6682 (2001).
- Boehm, M. *et al.* A growth factor-dependent nuclear kinase phosphorylates p27(Kip1) and regulates cell cycle progression. *EMBO J.* **21**, 3390–3401 (2002).
- McAllister, S. S., Becker-Hapak, M., Pintucci, G., Pagano, M. & Dowdy, S. F. Novel p27(Kip1) C-terminal scatter domain mediates Rac-dependent cell migration independent of cell cycle arrest functions. *Mol. Cell. Biol.* **23**, 216–228 (2003).
- Ishida, N., Kitagawa, M., Hatakeyama, S. & Nakayama, K. Phosphorylation at serine 10, a major phosphorylation site of p27(Kip1), increases its protein stability. *J. Biol. Chem.* **275**, 25146–25154 (2000).
- Kotake, Y., Nakayama, K., Ishida, N. & Nakayama, K. I. Role of serine 10 phosphorylation in p27 stabilization revealed by analysis of p27 knock-in mice harboring a serine 10 mutation. *J. Biol. Chem.* **280**, 1095–1102 (2005).
- Kawauchi, T., Chihama, K., Nabeshima, Y. & Hoshino, M. The *in vivo* roles of STEF/Tiam1, Rac1 and JNK in cortical neuronal migration. *EMBO J.* **22**, 4190–4201 (2003).
- Kawauchi, T., Chihama, K., Nishimura, Y. V., Nabeshima, Y. & Hoshino, M. MAP1B phosphorylation is differentially regulated by Cdk5/p35, Cdk5/p25, and JNK. *Biochem. Biophys. Res. Commun.* **331**, 50–55 (2005).
- Chae, T. *et al.* Mice lacking p35, a neuronal specific activator of Cdk5, display cortical lamination defects, seizures, and adult lethality. *Neuron* **18**, 29–42 (1997).
- Ishida, N. *et al.* Phosphorylation of p27Kip1 on serine 10 is required for its binding to CRM1 and nuclear export. *J. Biol. Chem.* **277**, 14355–14358 (2002).
- Connor, M. K. *et al.* CRM1/Ran-mediated nuclear export of p27(Kip1) involves a nuclear export signal and links p27 export and proteolysis. *Mol. Biol. Cell.* **14**, 201–213 (2003).
- Lee, M. H. *et al.* The brain-specific activator p35 allows Cdk5 to escape inhibition by p27Kip1 in neurons. *Proc. Natl Acad. Sci. USA* **93**, 3259–3263 (1996).
- Morisaki, H. *et al.* Cell cycle-dependent phosphorylation of p27 cyclin-dependent kinase (Cdk) inhibitor by cyclin E/Cdk2. *Biochem. Biophys. Res. Commun.* **240**, 386–390 (1997).
- Lacy, E. R. *et al.* Molecular basis for the specificity of p27 toward cyclin-dependent kinases that regulate cell division. *J. Mol. Biol.* **349**, 764–773 (2005).
- Tabata, H. & Nakajima, K. Multipolar migration: the third mode of radial neuronal migration in the developing cerebral cortex. *J. Neurosci.* **23**, 9996–10001 (2003).
- Noctor, S. C., Martinez-Cerdeno, V., Ivic, L. & Kriegstein, A. R. Cortical neurons arise in symmetric and asymmetric division zones and migrate through specific phases. *Nature Neurosci.* **7**, 136–144 (2004).
- Nikolic, M. The molecular mystery of neuronal migration: FAK and Cdk5. *Trends Cell Biol.* **14**, 1–5 (2004).
- Xie, Z., Sanada, K., Samuels, B. A., Shih, H. & Tsai, L. H. Serine 732 phosphorylation of FAK by Cdk5 is important for microtubule organization, nuclear movement, and neuronal migration. *Cell* **114**, 469–482 (2003).
- Gungabissoon, R. A. & Bamberg, J. R. Regulation of growth cone actin dynamics by ADF/cofilin. *J. Histochem. Cytochem.* **51**, 411–420 (2003).
- Moriyama, K., Iida, K. & Yahara, I. Phosphorylation of Ser-3 of cofilin regulates its essential function on actin. *Genes Cells* **1**, 73–86 (1996).
- Besson, A., Gurian-West, M., Schmidt, A., Hall, A. & Roberts, J. M. p27Kip1 modulates cell migration through the regulation of RhoA activation. *Genes Dev.* **18**, 862–876 (2004).
- Malek, N. P. *et al.* A mouse knock-in model exposes sequential proteolytic pathways that regulate p27Kip1 in G1 and S phase. *Nature* **413**, 323–327 (2001).
- Mitsuhashi, T. *et al.* Overexpression of p27Kip1 lengthens the G1 phase in a mouse model that targets inducible gene expression to central nervous system progenitor cells. *Proc. Natl Acad. Sci. USA* **98**, 6435–6440 (2001).
- Besson, A., Assoian, R. K. & Roberts, J. M. Regulation of the cytoskeleton: an oncogenic function for CDK inhibitors? *Nature Rev. Cancer* **4**, 948–955 (2004).
- Baldassarre, G. *et al.* p27(Kip1)-stathmin interaction influences sarcoma cell migration and invasion. *Cancer Cell* **7**, 51–63 (2005).
- Nagahama, H., Hatakeyama, S., Nakayama, K., Nagata, M. & Tomita, K. Spatial and temporal expression patterns of the cyclin-dependent kinase (CDK) inhibitors p27Kip1 and p57Kip2 during mouse development. *Anat. Embryol.* **203**, 77–87 (2001).
- Bai, J. *et al.* RNAi reveals doublecortin is required for radial migration in rat neocortex. *Nature Neurosci.* **6**, 1277–1283. Epub 2003 Nov 16 (2003).
- Gotz, M. Doublecortin finds its place. *Nature Neurosci.* **6**, 1245–1247 (2003).
- Corbo, J. C. *et al.* Doublecortin is required in mice for lamination of the hippocampus but not the neocortex. *J. Neurosci.* **22**, 7548–7557 (2002).
- Izawa, I., Amano, M., Chihara, K., Yamamoto, T. & Kaibuchi, K. Possible involvement of the inactivation of the Rho-Rho-kinase pathway in oncogenic Ras-induced transformation. *Oncogene* **17**, 2863–2871 (1998).
- Amano, M. *et al.* The COOH terminus of Rho-kinase negatively regulates rho-kinase activity. *J. Biol. Chem.* **274**, 32418–32424 (1999).
- King, C. C. *et al.* p21-activated kinase (PAK1) is phosphorylated and activated by 3-phosphoinositide-dependent kinase-1 (PDK1). *J. Biol. Chem.* **275**, 41201–41209 (2000).
- Yu, J. Y., DeRuiter, S. L. & Turner, D. L. RNA interference by expression of short-interfering RNAs and hairpin RNAs in mammalian cells. *Proc. Natl Acad. Sci. USA* **99**, 6047–6052 (2002).
- Matsuo, N., Hoshino, M., Yoshizawa, M. & Nabeshima, Y. Characterization of STEF, a guanine nucleotide exchange factor for Rac1, required for neurite growth. *J. Biol. Chem.* **277**, 2860–2868 (2002).
- Matsuo, N., Terao, M., Nabeshima, Y. & Hoshino, M. Roles of STEF/Tiam1, guanine nucleotide exchange factors for Rac1, in regulation of growth cone morphology. *Mol. Cell. Neurosci.* **24**, 69–81 (2003).
- Yoshizawa, M. *et al.* Involvement of a Rac activator, P-Rex1, in neurotrophin-derived signaling and neuronal migration. *J. Neurosci.* **25**, 4406–4419 (2005).
- Kioka, N. *et al.* Vincin: a novel vinculin-binding protein with multiple SH3 domains enhances actin cytoskeletal organization. *J. Cell Biol.* **144**, 59–69 (1999).

© 2006  nature publishing group

To order reprints, please contact:

In the Americas:

Tel 212 726 9233; Fax 212 679 0843; reprints@natureny.com

Europe/UK/ROW:

Tel + 44 (0)20 7843 4967; Fax + 44 (0)20 7843 4749; c.fothergill@nature.com

Japan & Korea:

Tel +81 3 3267 8751; Fax +81 3 3267 8746; reprints@naturejpn.com

Printed by The Friary Press, Dorchester, England.



MAP1B phosphorylation is differentially regulated by Cdk5/p35, Cdk5/p25, and JNK

Takeshi Kawauchi^a, Kaori Chihama^a, Yoshiaki V. Nishimura^a,
Yo-ichi Nabeshima^a, Mikio Hoshino^{a,b,*}

^a Department of Pathology and Tumor Biology, Graduate School of Medicine, Kyoto University, Kyoto 606-8501, Japan

^b Precursory Research for Embryonic Science and Technology (PRESTO), Japan Science and Technology Agency (JST), Kawaguchi 332-0012, Japan

Received 15 March 2005

Available online 30 March 2005

Abstract

Mode I phosphorylated MAP1B is observed in developing and pathogenic brains. Although Cdk5 has been believed to phosphorylate MAP1B in the developing cerebral cortex, we show that a Cdk5 inhibitor does not suppress mode I phosphorylation of MAP1B in primary and slice cultures, while a JNK inhibitor does. Coincidentally, an increase in phosphorylated MAP1B was not observed in COS7 cells when Cdk5 was cotransfected with p35, but this did occur with p25 which is specifically produced in pathogenic brains. Our primary culture studies showed an involvement of Cdk5 in regulating microtubule dynamics without affecting MAP1B phosphorylation status. The importance of regulating microtubule dynamics in neuronal migration was also demonstrated by in utero electroporation experiments. These findings suggest that mode I phosphorylation of MAP1B is facilitated by JNK but not Cdk5/p35 in the developing cerebral cortex and by Cdk5/p25 in pathogenic brains, contributing to various biological events.

© 2005 Elsevier Inc. All rights reserved.

Keywords: Microtubule-associated protein; MAP1B; Cdk5; p35; p25; Neuronal migration; Neurodegenerative disease; Alzheimer's disease; Roscovitine; SP600125

Microtubules play a crucial organizing role in neurons, conferring appropriate morphology on leading processes or neurites. The stability of microtubules is dynamically regulated, contributing to dynamic cellular events such as neuronal migration and neurite extension. At the tips of neuronal processes, which are in constant motion while searching for appropriate targets, dynamic rather than stable microtubules are principally observed [1]. Microtubule dynamics are thought to be regulated by microtubule-associated proteins (MAPs) in various cell types including neurons. One of the MAPs, MAP1B, is a microtubule-stabilizing phosphoprotein that is

expressed in the nervous system including radial migrating neurons in the developing cerebral cortex [2,3]. There are two phosphorylated forms of MAP1B; mode I phosphorylation which is detected only in the developing nervous system, and mode II phosphorylation which is observed throughout developmental stages and adulthood. It has been reported that MAP1B is phosphorylated at mode I sites by glycogen synthase kinase 3 β (GSK3 β) in cultured dorsal root ganglion cells, and that this results in a loss of the microtubule-stabilizing ability [4,5]. Mode I phosphorylated MAP1B is also observed in the neurofibrillary tangles (NFT) and dystrophic neurites (DN) in Alzheimer's diseased brains [6,7]. Furthermore, overexpression of MAP1B promotes not only neurite growth but also neuronal apoptosis [8]. These facts suggest that MAP1B and its phosphorylation are

* Corresponding author. Fax: +81 75 753 4676.

E-mail address: mikio@mls.med.kyoto-u.ac.jp (M. Hoshino).

involved in both the development and pathogenesis of the nervous system.

It has been suggested that proline-directed protein kinases (PDPKs) may phosphorylate MAP1B at mode I sites. Previously we reported that c-Jun N-terminal kinase (JNK), one of the PDPKs, is involved in mode I phosphorylation of MAP1B and neuronal migration in the developing cerebral cortex [9]. Another PDPK, cyclin-dependent kinase 5 (Cdk5), has also been implicated for involvement in mode I phosphorylation; antisense oligonucleotides for Cdk5 in cultured macro-neurons from the cerebellum were shown to decrease mode I phosphorylation of MAP1B [10,11]. However, direct evidence for Cdk5 involvement in MAP1B phosphorylation in the cerebral cortex is still lacking.

It has been known that Cdk5 requires its activator, p35, to exhibit kinase activity [12]. In pathological circumstances such as neurodegenerative disorders, p35 is processed to a more stable form, p25, which confers a stronger kinase activity upon Cdk5. Furthermore, it has been suggested that the substrate specificity and sub-cellular localization of p25 are distinct [13].

We show that Cdk5 is not involved in the phosphorylation of MAP1B at mode I sites in the developing cerebral cortex where p35, but not p25, is expressed. We also show that Cdk5 phosphorylates MAP1B at mode I sites only as a complex with p25, but not p35, in cultured cells. Furthermore, we show the importance of MAP1B regulation of microtubule stability in cortical neuronal migration through in utero electroporation experiments. These findings suggest that mode I phosphorylation of MAP1B is differentially regulated by Cdk5/p35, Cdk5/p25, and JNK in developing and pathogenic brains, contributing to a variety of physiological and pathologic events.

Experimental procedures

Plasmids. Plasmids were prepared using Endo Free plasmid purification kits (Qiagen). Oligonucleotides containing multicloning sites were inserted into pcCAG [9] to generate pCAG-MCS2. MAP1B [8], Cdk5 [14], p35 or p25 [15] cDNA was inserted into the pCAG-MCS2 vector. JNK expression vector was a generous gift from Dr. S. Tamura [16].

Antibodies and chemical reagents. Primary antibodies used in this study were SMI31 (Sternberger Monoclonals), anti-MAP1B (Santa Cruz N-19), anti-phospho-Ser732 FAK (Sigma), anti-FAK (Santa Cruz C-903), anti-activated JNK1/2 (Promega), anti-JNK1/2 (BD Biosciences), and anti-p35 (Santa Cruz C-19) antibodies. Roscovitine and SP600125 were purchased from Sigma and BIOMOL Research Laboratories, respectively.

Cell culture and transfection. COS7 cells were maintained in Dulbecco's modified Eagle's medium (Invitrogen) with 10% fetal bovine serum and antibiotics. Transfections were performed as described previously [17]. One molar D-sorbitol (Sigma) was added into the culture media for 30 min to activate JNK (Fig. 2).

In utero electroporation, primary culture, slice culture, and Western analyses. In utero electroporation, primary culture of E15 mouse

embryonic cortical neurons, slice culture of E16 mouse embryonic cortex, and Western analyses were performed as described previously [9,18].

Results and discussion

E15 cerebral cortices were dissociated and after 1 day in culture, inhibitors or solvent was added for another 24 h. Cells were harvested and subjected to immunoblot analysis with SMI31 antibody which recognizes mode I phosphorylated MAP1B [19]. As previously reported [9,20], treatment with a JNK inhibitor, SP600125, resulted in decreased mode I phosphorylation of MAP1B (Fig. 1A, SP25 and SP50). In contrast, treatment with a Cdk5 inhibitor, roscovitine, had no effect (Fig. 1A, R100), although this inhibitor decreased the phosphorylation of FAK at Ser732 (Fig. 1A, R100), which was reported to be phosphorylated by Cdk5 [21]. Interestingly, administration of a higher concentration of roscovitine (200 μ M) to the primary cortical culture increased the mode I phosphorylation of MAP1B (Fig. 1A, R200) and resulted in a nearly 6-fold increase of phosphorylated JNK1 at Thr and Tyr (Fig. 1B), corresponding to an activated JNK1 [22]. These results suggest that Cdk5 suppresses the activity of JNK1 as well as phosphorylation of MAP1B in cultured cortical neurons. Although it is possible that higher concentrations of roscovitine may affect the activity of molecules other than Cdk5, the report that Cdk5 inhibits JNK3 through the phosphorylation of Thr131 [23] suggests that the suppression of JNK1 activity may occur through similar molecular mechanisms.

To confirm these results in vivo, we used slice cultures of mouse E16 cerebral cortices in which many radially migrating neurons are observed [9]. To determine whether treatment with 100 μ M roscovitine can inhibit neuronal migration, we used enhanced GFP (EGFP) fluorescence to allow visualization of migrating neurons. Embryos were electroporated with EGFP expression vectors at E14 and coronal slices were taken at E16 and cultured for 20 h with or without 100 μ M roscovitine to observe the migration of GFP-positive cells. While GFP-positive cells migrated toward the pial surface in the control slices, roscovitine treatment inhibited cell migration, mimicking the cerebral cortex phenotype of Cdk5-deficient mice as well as that of dominant negative Cdk5-electroporated neurons (Fig. 1C) [9,24,25]. Consistent with this result, treatment with 100 μ M roscovitine to slice cultures resulted in suppression of FAK phosphorylation at Ser732 (Fig. 1D), suggesting that 100 μ M roscovitine inhibits Cdk5 kinase activity and Cdk5-dependent neuronal migration. However, treatment with 100 μ M roscovitine did not inhibit the mode I phosphorylation of MAP1B, while administration of 50 μ M SP600125 decreased this phosphorylation

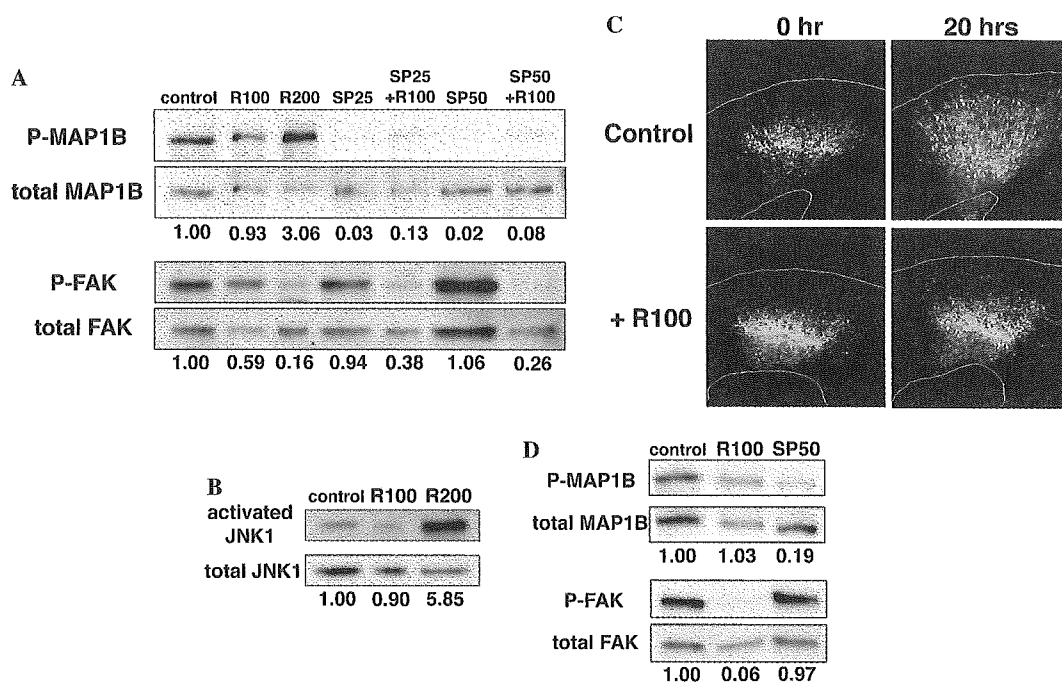


Fig. 1. Influence of roscovitine and SP600125 on the mode I phosphorylation of MAP1B and activation of JNK. (A) Primary cultures of E15 cerebral cortices (2DIV) were treated with 100 or 200 μ M roscovitine (R100 or R200), 25 or 50 μ M SP600125 (SP25 or SP50) or both (SP25 + R100 or SP50 + R100) for 24 h, and subjected to immunoblot analyses with SMI31 which recognizes mode I phosphorylated MAP1B (P-MAP1B), anti-MAP1B antibody (total MAP1B), anti-phospho-Ser732 FAK antibody (P-FAK) or anti-FAK antibody (total FAK). The numbers indicate the ratio of P-MAP1B/total-MAP1B and P-FAK/total-FAK, which were determined by chemiluminescence (FUJIFILM). While treatment with SP600125 resulted in decrease of the P-MAP1B/total-MAP1B ratio (SP25 and SP50), treatment with 100 μ M roscovitine had no effect (R100). Interestingly, the higher concentration of roscovitine (200 μ M) increased the ratio (R200). Addition of roscovitine to SP600125-treated cells caused a slight increase of P-MAP1B/total MAP1B ratio (SP25 + R100 and SP50 + R100). Similar results were obtained from five independent experiments. (B) Primary cultures of E15 cerebral cortices (2DIV) were treated with 100 or 200 μ M roscovitine (R100 or R200) or solvent (DMSO; control) for 24 h, and subjected to immunoblot analyses with anti-activated JNK1/2 or anti-JNK1/2 antibodies. JNK1 (46 kDa) signals are shown. In contrast to JNK1 signals, JNK2 (54 kDa) signals were very weak (data not shown). Experiments were performed in triplicate. (C) E14 brains were electroporated with EGFP expression vector and at E16, 300 μ m coronal sections were cultured on membrane inserts for 20 h with or without 100 μ M roscovitine (R100). Addition of 100 μ M roscovitine resulted in inhibition of neuronal migration. Similar results were obtained from five independent experiments. (D) Three hundred micrometers E16 coronal brain sections were cultured on membrane inserts for 24 h with 100 μ M roscovitine (R100), 50 μ M SP600125 (SP50) or solvent (DMSO; control). The numbers indicate the ratios of P-MAP1B/total-MAP1B and P-FAK/total-FAK, which were determined by chemiluminescence. Similar results were obtained from five independent experiments.

efficiently, suggesting that the phosphorylation of MAP1B mainly depends on JNK, but not Cdk5, in the developing cerebral cortex (Fig. 1D). These results suggest that Cdk5 regulates cortical neuronal migration through the phosphorylation of substrates other than MAP1B. Actually, Xie et al. reported that Cdk5 phosphorylates FAK, contributing to cortical neuronal migration [21,25]. Accordingly, in our experiments, 100 μ M roscovitine suppressed phosphorylation of FAK at Ser732 and consequently, neuronal migration. Although a high concentration of roscovitine (200 μ M) increased JNK activity (Fig. 1B), it also resulted in suppression of neuronal migration in this slice culture system (data not shown), exhibiting an effect indistinguishable from that of 100 μ M roscovitine shown in Fig. 1C. However, this result is not paradoxical, as it has previously been reported that increased activation of JNK by overexpression of MUK (MAPK-upstream protein kinase) perturbs cortical neuronal migration

[26]. Furthermore, overexpression of JNK by means of in utero electroporation also suppressed neuronal migration in vivo (our unpublished data). These facts may suggest that proper neuronal migration requires the appropriate activities of Cdk5 and JNK.

To further elucidate the ability of Cdk5 to phosphorylate MAP1B, we performed in vitro experiments using COS7 cells, in which Cdk5 activators, p35 and p25, were not detected by immunoblot analysis (data not shown). Because p35 was expressed in the embryonic cerebral cortex (Fig. 2A), COS7 cells were cotransfected with Cdk5 and p35 expression vectors, and subsequently subjected to immunoblotting with SMI31. A complex of Cdk5 with p35 was detected by immunoprecipitation from the transfected cells, suggesting that they can associate in COS7 cells (data not shown). However, expression of Cdk5/p35 resulted in little increase of phosphorylated MAP1B in the COS7 cells compared to the control cells transfected only with Cdk5, although

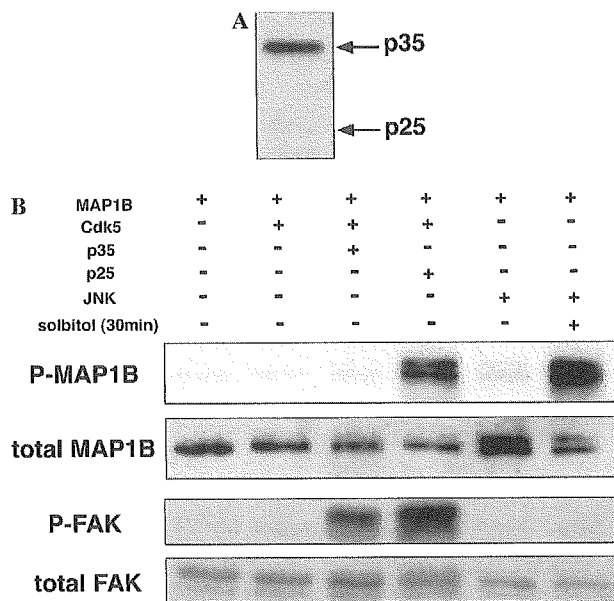


Fig. 2. Cdk5/p25 but not Cdk5/p35 phosphorylates MAP1B. (A) Immunoblot analysis of extract from E15 mouse embryonic cerebral cortex using an anti-p35 antibody (C-19, Santa Cruz), which recognizes both p35 and p25. This antibody recognizes both p35 and p25 in lysates from p35- or p25-transfected COS7 cells as well as brains with Alzheimer's disease (data not shown). (B) COS7 cells were cotransfected with the indicated plasmids and subsequently subjected to immunoblot analyses with SMI31 (P-MAP1B), anti-MAP1B (total MAP1B), anti-phospho-Ser732 FAK (P-FAK) or anti-FAK (total FAK) antibodies. Experiments were performed in quadruplicate.

Ser732 on FAK was strongly phosphorylated (Fig. 2B). This suggests that Cdk5 does not phosphorylate MAP1B when it associates with p35, consistent with the results in Fig. 1. In pathological circumstances such as neurodegenerative disorders, p35 is processed to a more stable form, p25 [13]. Only p35, not p25, is observed in the normal embryonic cerebral cortex (Fig. 2A). Because it has been suggested that Cdk5/p25 exhibits a substrate specificity distinct from Cdk5/p35 [13] and that mode I phosphorylated MAP1B and p25 are detected in brains with neurodegenerative disorders [6], we tested whether Cdk5/p25 phosphorylates MAP1B. Interestingly, when Cdk5 was cotransfected with p25, strong phosphorylation of MAP1B at mode I sites as well as FAK at Ser732 was detected (Fig. 2B). These facts suggest that Cdk5 phosphorylates MAP1B only upon association with p25, not with p35. Together with the result that JNK phosphorylates MAP1B in the embryonic cerebral cortex (Fig. 1), these findings suggest that mode I phosphorylation of MAP1B is facilitated by JNK but not Cdk5 in developing cerebral cortex, and further imply that Cdk5 may be involved in phosphorylation of MAP1B in p25-producing pathogenic brains.

Mode I phosphorylation of MAP1B is known to affect its ability to regulate microtubule dynamics [4]. However, whether proper regulation of microtubule dynamics is actually required for neuronal migration is

still unclear. Transfection of MAP1B into the primary cultured neurons of E15 cerebral cortex has been shown to significantly increase microtubule stability at the tips of the neuronal processes, confirming the positive effect of MAP1B on the microtubule stability in the transfected neurons (data not shown). We introduced MAP1B expression plasmids into ventricular zone cells of the mouse cerebral cortex at E14 using in utero electroporation. In control brains of P0 animals (5 days after electroporation), GFP-labeled transfected cells reached the superficial layer of the cortical plate as reported previously (Fig. 3A) [9]. However, in MAP1B-overexpressing brains, some of the transfected cells were found to stall in the intermediate zone, probably due to perturbed neuronal migration, although a portion of the transfected cells reached the superficial layer of the cortical plate (Fig. 3B). To estimate the extent of cell migration statistically, the fluorescence intensities in distinct layers of the electroporated cortex were recorded. $34.0 \pm 5.3\%$ of the EGFP fluorescence was detected in the cortical plate of cortices overexpressing MAP1B, compared to $78.1 \pm 4.9\%$ in the control cortices (Figs. 3C and D). This strongly suggests that proper regulation of microtubule dynamics is required for normal cortical neuronal migration.

While Cdk5 does not phosphorylate MAP1B in the developing cerebral cortex, it is known to phosphorylate several other microtubule-regulatory proteins [11,25].

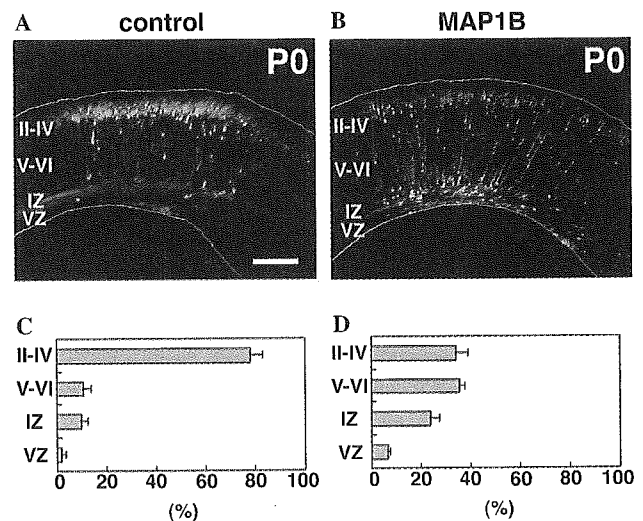


Fig. 3. Overexpression of MAP1B in the developing cerebral cortex. Control (A,C) or MAP1B expressing (B,D) vectors were transfected with pEGFP into E14 mouse embryonic brains by in utero electroporation. (A,B) At P0, 5 days after electroporation, frozen brain sections were examined for EGFP fluorescence. White lines represent pial and ventricular surfaces. (C,D) Estimation of cell migration by recording fluorescence intensities of EGFP in distinct regions of the cerebral cortex [9]. Each bar represents the mean percentage of relative intensity \pm SE $n = 6$. II–IV, layers II–IV of the cortical plate; V–VI, layers V–VI of the cortical plate; IZ, intermediate zone; VZ, ventricular zone. Scale bar: 200 μ m.

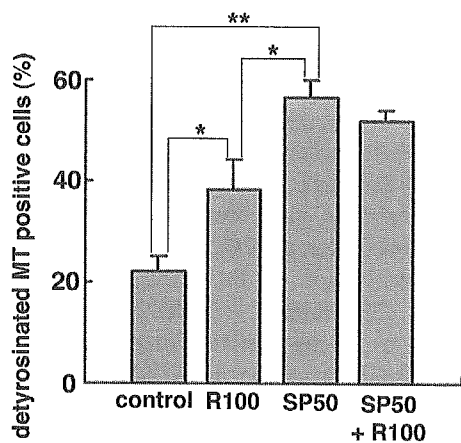


Fig. 4. E15 cerebral cortices were dissociated and cultured for 20 h, and subjected to an additional 8 h incubation with 100 μ M roscovitine (R100), 50 μ M SP600125 (SP50) or solvent (DMSO; control). Cells were stained with anti- α -tubulin and anti-detyrosinated tubulin antibodies, and the ratios of the cells containing detyrosinated microtubules at their process tips were determined. When the distance between the distal ends of detyrosinated microtubules and entire microtubules at the tip of the longest neurite was $<5 \mu$ m, that cell was counted as a 'detyrosinated MT-positive cell' [9]. Scores represent mean percentage \pm SE; $n = 5$ brains; * $p < 0.05$, ** $p < 0.02$, t test.

Because both the Cdk5 kinase activity and proper regulation of microtubule dynamics were required for normal neuronal migration (Figs. 1C and 3), we suspected that Cdk5 may influence microtubule stability to regulate neuronal migration. To test this, we investigated the effect of roscovitine treatment on microtubules in cultured cortical neurons. Primary cultured neurons were coimmunostained with anti-detyrosinated α -tubulin (a marker for stable microtubules) and anti- α -tubulin antibodies. Treatment with roscovitine significantly decreased detyrosinated microtubules at the tips of neuronal processes, indicating that Cdk5 can regulate microtubule dynamics without affecting the MAP1B phosphorylation status (Fig. 4). Cdk5 is known to phosphorylate PAK1 at Thr212 and this alters microtubule dynamics without affecting the kinase activity of PAK1 [27]. Therefore, Cdk5 may regulate microtubule dynamics at the tips of neuronal processes through phosphorylation of PAK1, although how the PAK1 activity controls the microtubule dynamics remains unclear.

Although Cdk5 is believed to phosphorylate MAP1B at mode I sites in the developing cerebral cortex [11,25], our results showed that this phosphorylation is dependent on JNK, not Cdk5. However, we also demonstrated that both Cdk5 and JNK are required for regulating microtubule dynamics and neuronal migration. These results suggest that these proline-directed protein kinases regulate different downstream pathways to control similar cellular events. On the other hand, the activities of both kinases can be regulated by the same upstream molecule, Rac1 [9,28]. These facts imply that

microtubule dynamics are complexly but coordinately regulated in the cerebral cortex during development.

Our experiments also suggest that Cdk5 suppresses mode I phosphorylation of MAP1B in developing cortical neurons, possibly through the inhibition of JNK activity. Furthermore, it was demonstrated that Cdk5 can phosphorylate MAP1B at mode I sites only when it associates with p25. These results suggest that conversion of p35 to p25 transforms Cdk5 from a negative regulator to a strong positive regulator for MAP1B phosphorylation. This conversion might be important in better understanding the pathology of neurodegenerative disorders, since both mode I phosphorylated MAP1B and p25 are frequently and abundantly observed in the neurofibrillary tangles of Alzheimer's disease [6,7,13,29].

Thus, mode I phosphorylation of MAP1B seems to be differentially regulated by Cdk5/p35, Cdk5/p25, and JNK in the developing as well as pathogenic brains. Further studies are required to understand the implications of MAP1B phosphorylation in the nervous system development and in neurodegenerative disorders.

Acknowledgments

We thank A. Takashima, S. Tamura, L.H. Tsai, and Y. Uchida for providing plasmids. We also thank R. Yu and M. Sone for helpful comments and technical help. This work was supported by the center of excellence (COE) grant and Grant-in-Aid for Scientific Research on Priority Areas, "Elucidation of glia–neuron network mediated information processing systems (#16047220)," and "Membrane Traffic (#16044225)" from the Ministry of Education, Culture, Sports and Science and Technology, Japan, and by grants from Japan Brain Foundation and Takeda Science Foundation.

References

- [1] T.B. Shea, Selective stabilization of microtubules within the proximal region of developing axonal neurites, *Brain Res. Bull.* 48 (1999) 255–261.
- [2] A. Cheng, B.K. Krueger, L.L. Bambrick, MAP5 expression in proliferating neuroblasts, *Brain Res. Dev. Brain Res.* 113 (1999) 107–113.
- [3] P.R. Gordon-Weeks, I. Fischer, MAP1B expression and microtubule stability in growing and regenerating axons, *Microsc. Res. Technol.* 48 (2000) 63–74.
- [4] R.G. Goold, R. Owen, P.R. Gordon-Weeks, Glycogen synthase kinase 3 β phosphorylation of microtubule-associated protein 1B regulates the stability of microtubules in growth cones, *J. Cell Sci.* 112 (1999) 3373–3384.
- [5] J.A. Del Rio, C. Gonzalez-Billault, J.M. Urena, E.M. Jimenez, M.J. Barallobre, M. Pascual, L. Pujadas, S. Simo, A. La Torre, F. Wandosell, J. Avila, E. Soriano, MAP1B is required for netrin 1 signaling in neuronal migration and axonal guidance, *Curr. Biol.* 14 (2004) 840–850.

- [6] L. Ulloa, E. Montejó de Garcini, P. Gomez-Ramos, M.A. Moran, J. Avila, Microtubule-associated protein MAP1B showing a fetal phosphorylation pattern is present in sites of neurofibrillary degeneration in brains of Alzheimer's disease patients, *Brain Res. Mol. Brain Res.* 26 (1994) 113–122.
- [7] M. Hasegawa, T. Arai, Y. Ihara, Immunochemical evidence that fragments of phosphorylated MAP5 (MAP1B) are bound to neurofibrillary tangles in Alzheimer's disease, *Neuron* 4 (1990) 909–918.
- [8] Y. Uchida, Overexpression of full-length but not N-terminal truncated isoform of microtubule-associated protein (MAP) 1B accelerates apoptosis of cultured cortical neurons, *J. Biol. Chem.* 278 (2003) 366–371, Epub 2002 Oct 2009.
- [9] T. Kawauchi, K. Chihama, Y. Nabeshima, M. Hoshino, The in vivo roles of STEF/Tiam1, Rac1 and JNK in cortical neuronal migration, *EMBO J.* 22 (2003) 4190–4201.
- [10] G. Pigino, G. Paglini, L. Ulloa, J. Avila, A. Caceres, Analysis of the expression, distribution and function of cyclin dependent kinase 5 (cdk5) in developing cerebellar macroneurons, *J. Cell Sci.* 110 (1997) 257–270.
- [11] S. Bielas, H. Higginbotham, H. Koizumi, T. Tanaka, J.G. Gleeson, Cortical neuronal migration mutants suggest separate but intersecting pathways, *Annu. Rev. Cell Dev. Biol.* 20 (2004) 593–618.
- [12] L.H. Tsai, I. Delalle, V.S. Caviness Jr., T. Chae, E. Harlow, p35 is a neural-specific regulatory subunit of cyclin-dependent kinase 5, *Nature* 371 (1994) 419–423.
- [13] G.N. Patrick, L. Zukerberg, M. Nikolic, S. de la Monte, P. Dikkes, L.H. Tsai, Conversion of p35 to p25 deregulates Cdk5 activity and promotes neurodegeneration, *Nature* 402 (1999) 615–622.
- [14] M. Nikolic, H. Dudek, Y.T. Kwon, Y.F. Ramos, L.H. Tsai, The cdk5/p35 kinase is essential for neurite outgrowth during neuronal differentiation, *Genes Dev.* 10 (1996) 816–825.
- [15] A. Takashima, M. Murayama, K. Yasutake, H. Takahashi, M. Yokoyama, K. Ishiguro, Involvement of cyclin dependent kinase5 activator p25 on tau phosphorylation in mouse brain, *Neurosci Lett.* 306 (2001) 37–40.
- [16] H. Wang, S. Ikeda, S. Kanno, L.M. Guang, M. Ohnishi, M. Sasaki, T. Kobayashi, S. Tamura, Activation of c-Jun amino-terminal kinase is required for retinoic acid-induced neural differentiation of P19 embryonal carcinoma cells, *FEBS Lett.* 503 (2001) 91–96.
- [17] N. Matsuo, M. Hoshino, M. Yoshizawa, Y. Nabeshima, Characterization of STEF, a guanine nucleotide exchange factor for Rac1, required for neurite growth, *J. Biol. Chem.* 277 (2002) 2860–2868.
- [18] N. Matsuo, M. Terao, Y. Nabeshima, M. Hoshino, Roles of STEF/Tiam1, guanine nucleotide exchange factors for Rac1, in regulation of growth cone morphology, *Mol. Cell. Neurosci.* 24 (2003) 69–81.
- [19] M. Johnstone, R.G. Goold, D. Bei, I. Fischer, P.R. Gordon-Weeks, Localisation of microtubule-associated protein 1B phosphorylation sites recognised by monoclonal antibody SMI-31, *J. Neurochem.* 69 (1997) 1417–1424.
- [20] C. Huang, K. Jacobson, M.D. Schaller, MAP kinases and cell migration, *J. Cell Sci.* 117 (2004) 4619–4628.
- [21] Z. Xie, K. Sanada, B.A. Samuels, H. Shih, L.H. Tsai, Serine 732 phosphorylation of FAK by Cdk5 is important for microtubule organization, nuclear movement, and neuronal migration, *Cell* 114 (2003) 469–482.
- [22] B. Derijard, M. Hibi, I.H. Wu, T. Barrett, B. Su, T. Deng, M. Karin, R.J. Davis, JNK1: a protein kinase stimulated by UV light and Ha-Ras that binds and phosphorylates the c-Jun activation domain, *Cell* 76 (1994) 1025–1037.
- [23] B.S. Li, L. Zhang, S. Takahashi, W. Ma, H. Jaffe, A.B. Kulkarni, H.C. Pant, Cyclin-dependent kinase 5 prevents neuronal apoptosis by negative regulation of c-Jun N-terminal kinase 3, *EMBO J.* 21 (2002) 324–333.
- [24] E.C. Gilmore, T. Ohshima, A.M. Goffinet, A.B. Kulkarni, K. Herrup, Cyclin-dependent kinase 5-deficient mice demonstrate novel developmental arrest in cerebral cortex, *J. Neurosci.* 18 (1998) 6370–6377.
- [25] M. Nikolic, The molecular mystery of neuronal migration: FAK and Cdk5, *Trends Cell. Biol.* 14 (2004) 1–5.
- [26] S. Hirai, A. Kawaguchi, R. Hirasawa, M. Baba, T. Ohnishi, S. Ohno, MAPK-upstream protein kinase (MUK) regulates the radial migration of immature neurons in telencephalon of mouse embryo, *Development* 129 (2002) 4483–4495.
- [27] M. Banerjee, D. Worth, D.M. Prowse, M. Nikolic, Pak1 phosphorylation on t212 affects microtubules in cells undergoing mitosis, *Curr. Biol.* 12 (2002) 1233–1239.
- [28] M. Nikolic, M.M. Chou, W. Lu, B.J. Mayer, L.H. Tsai, The p35/Cdk5 kinase is a neuron-specific Rac effector that inhibits Pak1 activity, *Nature* 395 (1998) 194–198.
- [29] H.C. Tseng, Y. Zhou, Y. Shen, L.H. Tsai, A survey of Cdk5 activator p35 and p25 levels in Alzheimer's disease brains, *FEBS Lett.* 523 (2002) 58–62.



Functional heterogeneity of side population cells in skeletal muscle

Akiyoshi Uezumi, Koichi Ojima, So-ichiro Fukada, Madoka Ikemoto, Satoru Masuda,
Yuko Miyagoe-Suzuki, Shin'ichi Takeda *

*Department of Molecular Therapy, National Institute of Neuroscience, National Center of Neurology and Psychiatry,
4-1-1 Ogawa-higashi, Kodaira, Tokyo 187-8502, Japan*

Received 18 December 2005
Available online 23 January 2006

Abstract

Skeletal muscle regeneration has been exclusively attributed to myogenic precursors, satellite cells. A stem cell-rich fraction referred to as side population (SP) cells also resides in skeletal muscle, but its roles in muscle regeneration remain unclear. We found that muscle SP cells could be subdivided into three sub-fractions using CD31 and CD45 markers. The majority of SP cells in normal non-regenerating muscle expressed CD31 and had endothelial characteristics. However, CD31⁺CD45⁺ SP cells, which are a minor subpopulation in normal muscle, actively proliferated upon muscle injury and expressed not only several regulatory genes for muscle regeneration but also some mesenchymal lineage markers. CD31⁺CD45⁺ SP cells showed the greatest myogenic potential among three SP sub-fractions, but indeed revealed mesenchymal potentials *in vitro*. These SP cells preferentially differentiated into myofibers after intramuscular transplantation *in vivo*. Our results revealed the heterogeneity of muscle SP cells and suggest that CD31⁺CD45⁺ SP cells participate in muscle regeneration.

© 2006 Elsevier Inc. All rights reserved.

Keywords: Side population cells; Muscle regeneration; Mesenchymal differentiation; Transplantation

Adult skeletal muscles have a remarkable ability to regenerate following muscle damage. This regeneration has been attributed to satellite cells that reside between the sarcolemma and the basal lamina. Satellite cells are quiescent mononucleated cells in normal conditions, however, in response to muscle damage, they become activated, proliferate, and then exit the cell cycle either to renew the quiescent satellite cell pool or to differentiate into mature myofibers. Thus, they have been considered to be the myogenic precursor cells that give rise to myoblasts and the sole source of adult myogenic cells [1].

In 1998, Ferrari et al. [2] have demonstrated for the first time that bone marrow (BM)-derived cells contribute to the skeletal muscle after BM transplantation. Side population (SP) cells were first identified in bone marrow based on the ability to exclude Hoechst 33342 dye as an enriched

fraction of hematopoietic stem cells (HSCs) [3]. Later, it has been reported that they also participate in muscle regeneration [4]. Studies using whole BM cells showed that BM-derived mononucleated cells display several characteristics of satellite cells, suggesting that donor-derived BM cells contribute to muscle fibers in a stepwise biological progression [5,6]. However, using single HSC transplantation experiment, Camargo et al. [7] suggested that cells committed to the myeloid lineage contribute to muscle through fusion event. Therefore, multiple mechanisms underlay contribution of BM-derived cells to skeletal muscle regeneration.

SP cells have been also identified in skeletal muscle [4]. Muscle SP cells cannot only reconstitute the hematopoietic system of lethally irradiated mice [4,8], but also differentiate into skeletal muscle cells [4,9]. Furthermore, they have been reported to participate in vascular regeneration [10]. Several lines of evidence suggest that muscle SP cells are a cell population distinct from satellite cells [9,11–13]. While muscle SP cells possess these attractive

* Corresponding author. Fax: +81 42 346 1750.
E-mail address: takeda@ncnp.go.jp (S. Takeda).

features, they have been reported to be heterogeneous population. In fact, muscle SP cells contain both CD45⁺ and CD45⁻ cells, and hematopoietic potential has been exclusively found in CD45⁺ fraction [8,9]. As regards the myogenic potential, both CD45⁺ and CD45⁻ fractions have been shown to differentiate into skeletal muscle cells [9,14], but there is no comparative study dealing with subpopulation of muscle SP cells during muscle regeneration.

In the present study, we have further divided muscle SP cells into three sub-fractions using CD31 and CD45, examined the properties of each sub-fraction, and identified a novel subpopulation (CD31⁻CD45⁻ SP cells) that showed the greatest myogenic potential both in vitro and in vivo. These results provide a new insight for stem cell-based therapy of muscular dystrophy.

Materials and methods

Animals. All procedures using experimental animals were approved by the Experimental Animal Care and Use Committee at the National Institute of Neuroscience. Eight- to ten-week-old C57BL/6 mice were purchased from Nihon CLEA (Japan). GFP Tg mice were provided by Dr. M. Okabe (Osaka University) and used in cell transplantation experiments. NOD/*scid* mice provided by the Institute for Experimental Animals, Japan, were used as recipients.

To induce muscle regeneration, 100 μ l of CTX (10 μ M in saline, Wako Chemicals) was injected into the tibialis anterior (TA) muscle with a 29-gauge needle. In FACS analysis experiments, CTX was injected into TA (50 μ l), gastrocnemius (50 μ l), and quadriceps femoris muscles (25 μ l).

BM transplantation was performed as previously described [14]. Mice were subjected to analysis 12 weeks after transplantation.

Antibodies. Mouse Bcrp-1 cDNA was provided by Dr. A.H. Schinkel [15]. A DNA fragment corresponding to cytoplasmic domain of Bcrp1, amino acids 300–337, was fused to GST in a pGEX-4T-2 vector (Amersham Biosciences), and the fusion protein was used to immunize rabbits. The serum obtained was affinity-purified. Other antibodies used in these studies are listed in Table S1.

Cell preparation and FACS analysis. Muscle-derived mononucleated cells were prepared from C57BL/6 mice, GFP Tg mice, or GFP-BM transplanted mice as previously described [14]. Hoechst staining was performed as described by Goodell et al. (http://www.bcm.tmc.edu/genetherapy/goodell/new_site/protocols.html). Cells were re-suspended at 10⁶ cells per ml in DMEM (Invitrogen) containing 2% FBS (Trace Biosciences), 10 mM Hepes, and 5 μ g/ml Hoechst 33342 (Sigma), and incubated for 90 min at 37 °C in the presence or the absence of 50 μ M verapamil (Sigma). During incubation, cells were mixed 3–4 times. For analysis of Ac-LDL uptake, 10 μ g/ml Dil-labeled Ac-LDL (Biomedical Technologies) was added. After antibody staining, cells were re-suspended in PBS containing 2.5% FBS and 2 μ g/ml propidium iodide (PI) (BD Pharmingen). Cell sorting was performed on a FACS VantageSE flow cytometer (BD Biosciences). Debris and dead cells were excluded by forward scatter, side scatter, and PI gating. Cell viability after staining and sorting was comparable to that previously reported [14].

RNA extraction and RT-PCR. Total RNA was extracted from 1 \times 10⁴ FACS sorted cells by using a RNeasy Micro Kit (Qiagen) and then reverse transcribed into cDNA by using TaqMan Reverse Transcription Reagents (Roche). The PCRs were performed with 1 μ l cDNA product under the following cycling conditions: 94 °C for 3 min followed by 40 cycles of amplification (94 °C for 15 s, 60 °C for 30 s, and 72 °C for 30 s) with a final incubation at 72 °C for 5 min. Specific primer sequences used for PCR are available on request.

Cell culture. SP cells were cultured alone with growth medium (GM); DMEM containing 20% FBS and 2.5 ng/ml bFGF (Invitrogen) in chamber slides (Nalge Nunc) coated with Matrigel (BD Biosciences) for 3–5 days. For osteogenic differentiation, the medium was changed to a differentiation medium (DM), 5% horse serum in DMEM supplemented with or without 500 ng/ml recombinant human BMP2 (R&D Systems), and cultured for 4–6 days. For adipogenic differentiation, cells were exposed to 3 cycles of 3 days of adipogenic induction medium (Cambrex Bioscience) followed by 1 day of adipogenic maintenance medium (Cambrex Bioscience) and then cells were maintained for five more days in the adipogenic maintenance medium. Alkaline phosphatase (AP) was stained using Sigma kit #85 according to the manufacturer's instructions. To stain lipids, cells were fixed in 10% formalin, rinsed in water and then 60% isopropanol, stained with Oil red O in 60% isopropanol, and rinsed in water. For myogenic differentiation, muSP-31, muSP-45, or muSP-DN purified from GFP Tg mice were co-cultured with myoblasts prepared from C57BL/6 mice as previously described [16,17] in GM. DM was supplied 3–5 days after starting co-culture.

Osteogenic activity and myotube-forming activity were determined by the following formulas: osteogenic activity = [the number of AP⁺ cells in seven randomly selected fields (corresponding to one-tenth of the whole area of the well)]/(the number of seeded cells) and myotube-forming activity = [(the number of GFP⁺ myotubes in seven randomly selected fields)]/(the number of seeded cells). In order to measure the extent of adipogenic differentiation, stained oil droplets were extracted for 5 min with 100 μ l of 4% Nonidet P-40 in isopropanol, and the absorbance of the dye-triglyceride complex was measured at 520 nm [18]; then, adipogenic activity was determined by the following formula: (the absorbance at 520 nm)/(the number of seeded cells).

Intramuscular transplantation experiments. muSP-DN or muSP-31 cells were purified from GFP Tg mice and were injected directly into the TA muscles of NOD/*scid* mice. One day before transplantation, host TA muscles were treated with CTX. The number of transplanted cells is indicated in Table 1. Three weeks after transplantation, TA muscles were excised and fixed in 4% PFA for 30 min, immersed sequentially in 10% sucrose/PBS and 20% sucrose/PBS, and frozen in isopentane cooled with liquid nitrogen.

Immunohistochemistry. FACS sorted cells were collected by Cytospin3 (ThermoShandon). Cells were fixed with 4% PFA for 5 min. Frozen muscle tissues were sectioned using a cryostat. Specimens were blocked with 5% goat serum (Cedarlane) in PBS for 15 min and incubated with primary antibodies at 4 °C overnight, followed by secondary staining. Stained cells were mounted in Vectashield with DAPI (Vector) and photographed using a fluorescence microscope IX70 (OLYMPUS) equipped with a QuantixTM air-cooled CCD camera (Photometrics) and IP Lab software (Scanalytics Inc.). Stained muscle sections were counterstained with TOTO-3 (1:5000; Molecular Probes), then mounted in Vectashield (Vector), and observed under the confocal laser scanning microscope system TCSSP (Leica).

Statistics. Values were expressed as means \pm SD or \pm SEM. Statistical significance was assessed by Student's *t* test. In comparison of more than two groups, one-way analysis of variance (ANOVA) followed by the Fisher's PLSD was used. A probability of less than 5% ($P < 0.05$) or 1% ($P < 0.01$) was considered statistically significant.

Table 1
Appearance of GFP⁺ myofibers after intramuscular transplantation

Cell type	Experiment No.	Number of injected cells/TA muscle	Number of GFP ⁺ myofibers/TA muscle
muSP-DN cells	Ex. 1	1.7 \times 10 ³	14
	Ex. 2	2.5 \times 10 ³	9
	Ex. 3	2.5 \times 10 ³	0
muSP-31 cells	Ex. 1	1.6 \times 10 ⁴	3
	Ex. 2	1.6 \times 10 ⁴	0
	Ex. 3	1.6 \times 10 ⁴	0

Results

Most muscle SP cells are found in a subset of capillary or vein endothelial cells in non-regenerating skeletal muscle

We identified verapamil-sensitive SP cells in skeletal muscle after Hoechst staining (Fig. 1A) and analyzed the expression of several markers on them. The majority of muscle SP cells were CD31⁺, usually recognized as a marker of endothelial cells (Figs. 1B–E), and negative for a pan-hematopoietic marker, CD45 (Fig. 1B). More than half of muscle SP cells were CD34⁺, and Sca-1⁺ cells comprised 90% of muscle SP cells (Figs. 1C and D). Compared to FACS profiles of whole-muscle-derived cells, SP cells were enriched in Sca-1⁺ cells (Fig. S1). More than 85% of muscle SP cells were CD31⁺ and took up acetylated low-density lipoprotein (Ac-LDL), a functional marker for endothelial cells and macrophages (Fig. 1E). These results indicate that most muscle SP cells have endothelial characteristics. Only cells in the main population (MP) were found to be Pax7⁺, indicating that SP cells do not include muscle satellite cells (data not shown).

To examine the localization of muscle SP cells, we generated a rabbit polyclonal anti-mouse Bcrp1 antibody, because it has been reported that Bcrp1 is the major determinant of the SP phenotype [19]. Our antibody clearly recognized Bcrp1 expression in liver, small intestine, and kidney, as previously reported (Fig. S2) [20,21]. We confirmed that Bcrp1 antibody recognizes more than 80% of SP cells and less than 3% of MP cells collected by cytopsin (Figs. 1F and G). In skeletal muscle, Bcrp1⁺ cells were found outside the muscle basal lamina (Fig. 1H), which clearly distinguished Bcrp1⁺ cells from satellite cells. Next, Bcrp1 expression in the vascular system was investigated. CD31 staining identified all endothelia from larger vessels to capillaries in muscle sections. Intriguingly, Bcrp1 was expressed by CD31-expressing endothelial cells, and its expression was preferentially observed on a subpopulation of capillary endothelium (Figs. 1I–K) and venous endothelium surrounded by thin vessel walls, as revealed by α -smooth muscle actin (α SMA) expression (Figs. 1L–N). These results, together with the results of FACS analysis, strongly suggest that the majority of muscle SP cells are a subset of endothelial cells present in capillaries or veins in non-regenerating skeletal muscle.

Behavior of muscle SP cells during muscle regeneration

We next examined the kinetics of SP cells during muscle regeneration induced by injection of cardiotoxin (CTX). After CTX injection, the total number of mononuclear cells per muscle weight gradually increased, with a peak at day 3. The number of SP cells also increased and reached its peak at day 3 (Fig. 2A). Muscle SP cells could be divided into three subpopulations based on CD31 and CD45 expression: CD31⁺CD45⁻ SP cells (designated muSP-31 cells), CD31⁻CD45⁺ SP cells (muSP-45 cells), and

CD31⁻CD45⁻ SP cells (muSP-DN cells), muSP-31 cells and muSP-DN cells distributed throughout the SP tail, but muSP-45 cells were located close to the shoulder (data not shown). The majority of muscle SP cells in untreated muscle were muSP-31 cells (Fig. 1B). During regeneration, however, muSP-45 cells and muSP-DN cells increased in both their ratios and their numbers (Figs. 2B and C). Although CD45⁺ cells were abundant in whole muscle-derived cells during regeneration and most of them were F4/80 antigen-positive mature macrophages, SP cells did not contain any mature inflammatory cells, as previously reported (data not shown) [14].

To clarify the origin of each subpopulation of SP cells, BM transplantation experiments were performed. We confirmed that muSP-45 cells were mobilized from bone marrow as previously reported (Figs. 3A and B) [14]. In contrast, both CD45⁻ SP fractions are residents of skeletal muscle (Figs. 3A and B), consistent with the results reported by Rivier et al. [22].

Next, to determine whether each subpopulation of SP cells proliferates in damaged muscle, cells were stained with Ki67 antibody. Most muSP-45 cells (Figs. 3C and D) and muSP-31 cells (Figs. 3G and H) prepared from regenerating muscle were negative for Ki67, suggesting that the proliferation activities of these two fractions were low. On the other hand, about 60% of muSP-DN cells were positive for Ki67 (Figs. 3E and F), indicating that muSP-DN cells actively proliferated during muscle regeneration.

We next examined Bcrp1 expression on three sub-fractionated SP cells and found that only muSP-31 cells were Bcrp1-positive (Fig. 3K). These results suggest that some ABC transporters other than Bcrp1 are responsible for the phenotype of CD31⁻ SP cells.

Gene expression of muscle SP cells during muscle regeneration

Our analysis revealed that each subpopulation of SP cells showed distinct kinetics during muscle regeneration. To better understand the traits of muscle SP cells, we analyzed gene expression during muscle regeneration. Three subpopulations of SP cells (in following experiments, muSP-45 cells from untreated muscle were omitted because of their low yield) or MP cells were collected from each time point during muscle regeneration, and RT-PCR was performed. We chose several myogenic (*Pax3*, *Pax7*, and *myf5*), endothelial (*Tie2*, *Flk1*, and *vWF*), and mesodermal-mesenchymal-associated (α SMA, *PPAR γ* , *Runx2*, *PDGFR α* , and *PDGFR β*) genes to clarify lineage characteristics of the target cells. We also examined expression of genes of developmental regulators (*msx1*, *Frizzed4* (*Fzd4*), *Patched1* (*Ptc1*), and *BMPRIA*), angiogenic factors (*angiopoietin-1* (*ang1*) and *VEGF*), and TGF- β superfamily antagonists (*folliclestatin* and *DAN*). muSP-DN cells from untreated muscles expressed only *PDGFR β* , *Ptc1*, *ang1*, *folliclestatin*, and *DAN* (Fig. 4, cont. lane 1). Neither myogenic nor other lineage-specific markers could be detected in

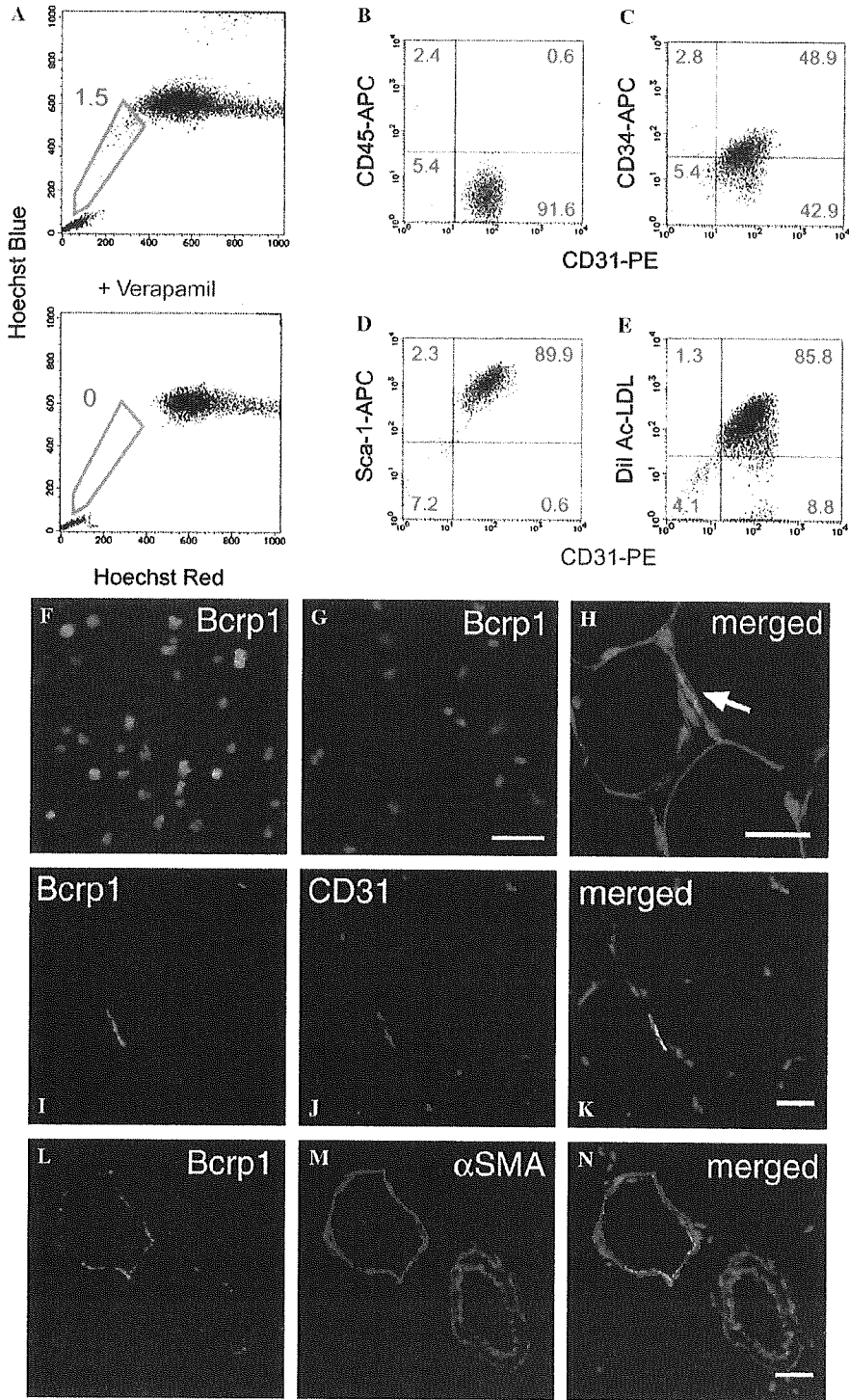


Fig. 1. Characterization of skeletal muscle SP cells. (A) Flow cytometric analysis of muscle-derived mononucleated cells after Hoechst 33342 staining with (lower panel) or without Verapamil (upper panel). The numbers indicate the percentage of SP cells (blue pentagons) in all mononucleated cells. (B–E) The expression of CD45 (B), CD34 (C), Sca-1 (D), and Dil-Ac-LDL uptake (E), and CD31 (B–E) on muscle SP cells. The percentage of cells in each quadrant is shown in the panel. (F,G) Immunofluorescent staining for Bcrp1 (green) and DAPI counterstaining (blue) of freshly sorted SP (F) and MP (G) cells. Immunofluorescent staining for Bcrp1 (green) and laminin $\alpha 2$ chain (red) (H), Bcrp1 (green) and CD31 (red) (I–K), and Bcrp1 (green) and α -smooth muscle actin (red) (L–N). TOTO-3 nuclear staining is shown in merged images (blue in H, K, and N). Bcrp1-positive cells are located outside the basal lamina (arrow), and they are partially overlapped with endothelial cells of capillary (I–K) and vein (L–N). Bars: 50 μ m in (F,G), 20 μ m in (H–N).

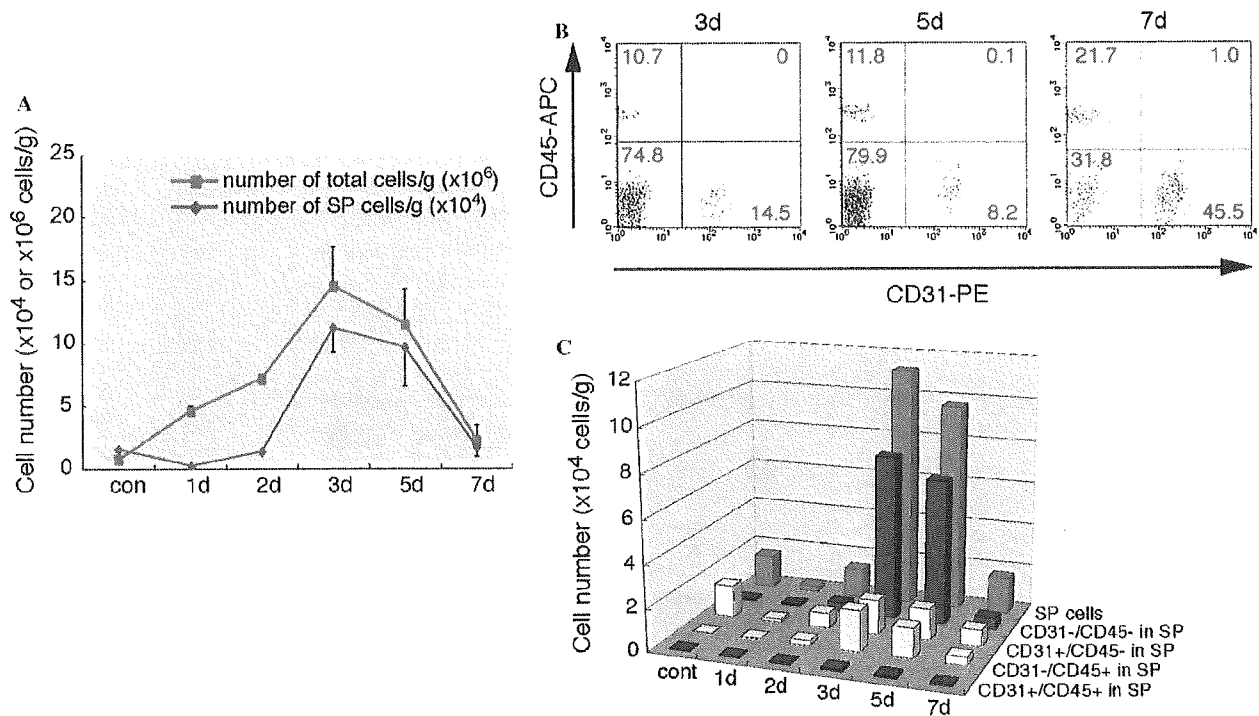


Fig. 2. Behavior of subpopulations of SP cells during muscle regeneration. (A) At 1 day (1d), 2 days (2d), 3 days (3d), 5 days (5d), and 7 days (7d) after CTX injection, the number of total cells (pink line) and SP cells (blue line) per gram of muscle weight was quantified. (B) At 3 days (3d), 5 days (5d), and 7 days (7d) after CTX injection, muscle SP cells prepared from regenerating muscle were analyzed for CD31 and CD45 expression. (C) Cell numbers in subpopulations of SP cells. muSP-45 cells (light blue bar) and muSP-DN cells (dark red bar) were significantly increased in number during muscle regeneration. Values (A,C) are the average of three independent experiments. Error bars represent SD.

this population indicating that muSP-DN cells do not contain cells committed to the lineages tested. At day 3 after CTX injection, muSP-DN cells began to express developmental regulator genes (Fig. 4, 3d, lane 1), and then at day 5, they also began to express several other lineage-specific genes (*Tie2*, α *SMA*, *PPAR γ* , and *Runx2*). Angiogenic factors and TGF- β superfamily antagonists were also strongly expressed at this time point (Fig. 4, 5d, lane 1). In contrast, muSP-31 cells continuously expressed all three endothelial genes analyzed throughout the regeneration process (Fig. 4, lane 2). Expression of mature endothelial marker, such as *vWF*, suggests that muSP-31 cells represent committed endothelial cells. muSP-45 cells expressed only low levels of α *SMA*, *PDGFR β* , and *follistatin* at day 5 after CTX injection (Fig. 4, lane 3). Myogenic markers, *Pax7* and *myf5*, were detected only in the MP fraction (Fig. 4, MP) indicating that myogenic cells are completely sorted into the MP fraction even during the process of muscle regeneration.

Differentiation potential of muscle SP cells for mesenchymal lineages

muSP-DN cells showed a unique gene expression pattern during muscle regeneration process: they began to express several mesenchymal genes at a late phase of muscle regeneration. Therefore, we examined the mesenchymal

potentials of muscle SP subpopulations. muSP-DN cells from untreated muscle readily gave rise to alkaline phosphatase (AP)-positive cells when cultured in the presence of bone morphogenetic protein 2 (BMP2) (Figs. 5A and C). With adipogenic induction, they also differentiated into adipocytes containing numerous lipid droplets in the cytoplasm (Figs. 5A and D). Reflecting the results of gene expression analysis, muSP-DN cells from regenerating muscle more efficiently differentiated into osteogenic cells and adipocytes than those from untreated muscle did (Figs. 5B–D). Unexpectedly, muSP-DN cells from regenerating muscle also differentiated into adipocytes without adipogenic induction (Figs. 5B and D), suggesting that they are susceptible to adipogenesis under our culture condition. In contrast, muSP-31 cells did not possess these differentiation potentials (Figs. 5A–D). Nor did muSP-45 cells, which were dramatically mobilized from BM into regenerating muscle (Figs. 5B–D). The attribute of differentiation potential is therefore a feature of muSP-DN.

Myogenic potential of muscle SP cells in vitro

We next evaluated the myogenic potential of muscle SP cells in vitro. When SP cells were cultured alone, they never differentiated into skeletal muscle cells (data not shown). Each subpopulation of SP cells was prepared from GFP Tg mice and co-cultured with wild type (WT) primary